Helsinki University of Technology
Department of Biomedical Engineering and Computational Science Publications
Teknillisen korkeakoulun Lääketieteellisen tekniikan ja laskennallisen tieteen laitoksen julkaisuja
October, 2008 REPORT A03

PROCESSING OF WEAK MAGNETIC MULTICHANNEL SIGNALS: THE SIGNAL SPACE SEPARATION METHOD

Samu Taulu

Dissertation for the degree of Doctor of Science in Technology to be presented with due permission of the Faculty of Information and Natural Sciences, Helsinki University of Technology, for public examination and debate in Auditorium N at Helsinki University of Technology (Espoo, Finland) on the 8th of October, 2008, at 12 noon.

Helsinki University of Technology
Faculty of Information and Natural Sciences
Department of Biomedical Engineering and Computational Science

Teknillinen korkeakoulu
Informaatio- ja luonnontieteiden tiedekunta
Lääketieteellisen tekniikan ja laskennallisen tieteen laitos

Distribution:
Helsinki University of Technology
Department of Biomedical Engineering and Computational Science
P.O.Box 9203
FI-02015 TKK
FINLAND

Tel. +358 9 451 3172
Fax +358 9 451 3182
http://www.becs.tkk.fi

Online pdf format: http://lib.tkk.fi/Diss/2008/isbn9789512295654/

E-mail: Samu.Taulu@neuromag.fi

ISBN 978-951-22-9564-7 (printed)
ISBN 978-951-22-9565-4 (pdf)
ISSN 1797-3996

Picaset Oy
Helsinki 2008

ABSTRACT OF DOCTORAL DISSERTATION	HELSINKI UNIVERSITY OF TECHNOLOGY P. O. BOX 1000, FI-02015 TKK http://www.tkk.fi

Author Samu Taulu

Name of the dissertation

Processing of weak magnetic multichannel signals: The signal space separation method

Manuscript submitted 31.03.2008	Manuscript revised 03.07.2008
Date of the defence 08.10.2008	
☐ Monograph	☒ Article dissertation (summary + original articles)

Faculty	Faculty of Information and Natural Sciences
Department	Department of Biomedical Engineering and Computational Science
Field of research	Applied mathematics and neuroscience
Opponent(s)	Dr. Seppo Ahlfors
Supervisor	Prof. Risto Ilmoniemi
Instructor	Dr. Juha Simola

Abstract

This work concentrates on processing of multichannel magnetoencephalographic (MEG) data. The aim of the work is to improve the quality of the measured signals in order to enable reliable data analysis. A special requirement for the developed mathematical methods is that they should be applicable to all MEG measurements regardless of the level of cooperation of the subject. This is essential, e.g., with small children and in clinical investigations. In addition to MEG, the methods presented here can be used in other magnetic multichannel measurements, too.

MEG measurements are used in basic brain research and recently also in clinical examinations. The method has excellent time resolution and reasonably good spatial resolution, which makes it a very useful tool in analysis of various brain functions. During the last 20 years, the instrumentation of MEG has been developed from devices containing less than 40 channels and limited coverage to whole-head systems with more than 300 channels. Yet, many of the signal processing and analysis methods used today date back to the time of the old instrumentation with limited coverage of the magnetic field.

Traditionally, MEG investigations have been performed primarily only with cooperative subjects in order to avoid the characteristic problems of MEG, including signal distortions due to head movements and artifacts caused by sources attached to the body. In clinical measurements, however, the patient may have involuntary movements and carry artifact sources such as therapeutic stimulators.

This work introduces the signal space separation method (SSS), which is based on Maxwell's equations and the generous spatial sampling by modern multichannel MEG devices. The thesis describes the theoretical foundations of SSS and its temporal extension tSSS, and demonstrates the results in several applications. SSS and tSSS are shown to significantly improve the quality of MEG data under conditions previously considered too challenging for meaningful analysis. Notably, the methods have potential to expand the applicability of MEG to some new patient groups, e.g., patients with deep brain stimulators.

Keywords	magnetoencephalography, signal processing, multichannel measurement, clinical applications
ISBN (printed) 978-951-22-9564-7	ISSN (printed) 1797-3996
ISBN (pdf) 978-951-22-9565-4	ISSN (pdf)
Language English	Number of pages 68 p. + app. 84 p.
Publisher	Depart. of Biomedical Engineering and Computational Science, Helsinki Univ. of Technology
Print distribution	Depart. of Biomedical Engineering and Computational Science, Helsinki Univ. of Technology
☒ The dissertation can be read at http://lib.tkk.fi/Diss/2008/isbn9789512295654	

VÄITÖSKIRJAN TIIVISTELMÄ	TEKNILLINEN KORKEAKOULU PL 1000, 02015 TKK http://www.tkk.fi

Tekijä Samu Taulu

Väitöskirjan nimi

Heikkojen magneettisten monikanavamittausten käsittely signaaliavaruuserottelumenetelmällä

Käsikirjoituksen päivämäärä 31.03.2008	Korjatun käsikirjoituksen päivämäärä 03.07.2008
Väitöstilaisuuden ajankohta 08.10.2008	
☐ Monografia	☒ Yhdistelmäväitöskirja (yhteenveto + erillisartikkelit)

Tiedekunta	Informaatio- ja luonnontieteiden tiedekunta
Laitos	Lääketieteellisen tekniikan ja laskennallisen tieteen laitos
Tutkimusala	Sovellettu matematiikka ja neurotiede
Vastaväittäjä(t)	TkT Seppo Ahlfors
Työn valvoja	Prof. Risto Ilmoniemi
Työn ohjaaja	TkT Juha Simola

Tiivistelmä

Tämä työ keskittyy magnetoenkefalografian (MEG) signaalinkäsittelyyn. Työn tarkoituksena on parantaa mitattujen signaalien laatua luotettavan data-analyysin varmistamiseksi. Kehitettyjen matemaattisten menetelmien erityisvaatimuksena on, että niiden pitää olla sovellettavissa kaikkiin MEG-mittauksiin riippumatta koehenkilön yhteistyöstä. Tämä on erityisen tärkeää esimerkiksi pieniä lapsia ja potilaita koskevissa tutkimuksissa. MEG:n lisäksi työssä esitetyt menetelmät ovat sovellettavissa muihin monikanavamittauksiin.

MEG-mittauksia käytetään aivojen perustutkimuksessa ja nykyään myös kliinisissä tutkimuksissa. Menetelmällä on erinomainen aika- ja tyydyttävä paikkatarkkuus, mikä tekee MEG:stä erittäin hyödyllisen työkalun erilaisten aivotoimintojen analysoimisessa. Viimeisten kahdenkymmenen vuoden aikana MEG-laitteistot ovat kehittyneet alle 40-kanavaisista, pään rajoitetusti kattavista laitteista yli 300-kanavaisiksi koko pään kattaviksi järjestelmiksi. Tästä huolimatta monet nykyään käytössä olevat signaalinkäsittelymenetelmät on kehitetty aikana, jolloin aivojen tuottamaa magneettikenttää ei vielä pystytty mittaamaan kattavasti.

Perinteisesti MEG-tutkimuksia on suoritettu etupäässä yhteistyökykyisille koehenkilöille MEG:n tyypillisten ongelmien välttämiseksi. Näihin ongelmiin kuuluvat esimerkiksi pään liikkeen ja kehossa olevien häiriölähteiden aiheuttamat signaalivääristymät. Kuitenkin kliinisissä mittauksissa potilaalla voi esiintyä tahdosta riippumattomia liikkeitä ja hänellä voi olla häiriötä tuottavia lähteitä, kuten hoidossa käytettäviä stimulaattoreita.

Tässä työssä esitellään signaaliavaruuserottelumenetelmä (SSS), joka pohjautuu nykyaikaisten MEG-laitteiden kattavaan kenttänäytteistykseen ja Maxwellin yhtälöihin. Väitöskirjassa kuvataan SSS:n ja sen ajallisen laajennuksen tSSS:n teoreettiset perusteet ja esitellään tuloksia useissa sovelluksissa. Työssä osoitetaan, että SSS ja tSSS parantavat merkittävästi MEG-signaalien laatua tilanteissa, joita on perinteisesti pidetty liian haastavina mielekkään analyysin kannalta. Erityisesti näytetään, että menetelmillä on mahdollisuus laajentaa MEG-tutkimukset koskemaan uusia potilasryhmiä, kuten syväaivostimulaattoreilla hoidettavia potilaita.

Asiasanat magnetoenkefalografia, signaalinkäsittely, monikanavamittaus, kliiniset sovellukset	
ISBN (painettu) 978-951-22-9564-7	ISSN (painettu) 1797-3996
ISBN (pdf) 978-951-22-9565-4	ISSN (pdf)
Kieli Englanti	Sivumäärä 68 s. + liit. 84 s.
Julkaisija Lääketieteellisen tekniikan ja laskennallisen tieteen laitos, Teknillinen korkeakoulu	
Painetun väitöskirjan jakelu Lääketieteellisen tekniikan ja laskennallisen tieteen laitos, Teknillinen korkeakoulu	
☒ Luettavissa verkossa osoitteessa http://lib.tkk.fi/Diss/2008/isbn9789512295654	

Academic dissertation

Processing of weak magnetic multichannel signals: The signal space separation method

Author:	Samu Taulu Elekta Neuromag Oy Helsinki, Finland
Supervising professor:	Prof. Risto Ilmoniemi Department of Biomedical Engineering and Computational Science Helsinki University of Technology Espoo, Finland
Supervisor:	Dr. Juha Simola Elekta Neuromag Oy Helsinki, Finland
Preliminary examiners:	Prof. Jari Kaipio Department of Applied Physics University of Kuopio Kuopio, Finland Dr. Guido Nolte Fraunhofer FIRST Berlin, Germany
Official opponent:	Assist. Prof. Seppo Ahlfors Harvard Medical School MGH/MIT/HMS Athinoula A. Martinos Center for Biomedical Imaging Charlestown, Massachusetts, U.S.A.

Preface and acknowledgements

This thesis was carried out in Elekta Neuromag Oy (formerly Neuromag Oy) and the results represent my vision of efficient method development work in a high technology company. I have been extremely fortunate to have the chance of working in an environment with highly professional colleagues in the company, a large network of world-class scientists as collaborators, and excellent tools for conducting my work. Based on my experience, a commercial company aiming at developing new methods and techniques in a quickly developing field, such as MEG, requires courage to break the strict traditional role models between industrial and academic institutions. Most importantly, efficient development can only be accomplished by people excited about their work and willing to take personal responsibility that goes beyond fulfilling predetermined tasks within given working hours. I am grateful to Dr. Antti Ahonen, the long-term managing director of Neuromag Oy and the present head of research and customer relations at Elekta Neuromag Oy, for creating an informal and enthusiastic atmosphere where everybody is given an equal chance to perform and where the actual results of the work matter.

I am most grateful to my instructor Dr. Juha Simola who is a brilliant physicist and a very important mentor for me. Our collaboration has been very fruitful from the beginning and he has really affected the way I think and approach mathematical problems. He is always very encouraging and never gets tired of creating new innovations and seeing progress by his colleagues. I have always felt that he is truly interested in my work and exited about the results that we have achieved together. In addition, he lifts the spirits of the whole working environment by his great sense of humour.

My scientific career started at the Low Temperature Laboratory of Helsinki University of Technology and I have greatly benefited from experiencing the creative and efficient way of working in this famous laboratory. Especially, I wish to thank the head of the Low Temperature Laboratory, Prof. Mikko Paalanen, for giving me the possibility to work there. I would also like to thank Prof. Riitta Hari, the head of the Brain Research Unit, for actively contributing to my thesis as a co-author. Our collaboration has been very fluent and it has helped me to confirm the theoretical part of my work by relevant neuroscientific demonstrations.

I would like to thank my co-author and close colleague Mr. Matti Kajola for many lively and stimulating discussions about all kinds of mathematical methods. Our mutual conversations and the associated computer simulations laid the foundation to the basic theory of my thesis. I am also grateful to Mr. Lauri Parkkonen for kindly and patiently guiding me into the world of MEG during my undergraduate studies, and for his continuous help and support ever after. I wish to thank Prof. Matti Hämäläinen for the motivating teaching of mathematics and algorithms of MEG in

the beginning of my career. I wish to express my gratitude to Dr. Jukka Nenonen for joyful collaboration and his invaluable contribution in designing and implementing the computer algorithms based on the methods developed in this thesis work.

I am grateful to the preliminary examiners Prof. Jari Kaipio and Dr. Guido Nolte for reviewing the thesis in detail and giving comments that helped me to improve it and make it more readable. I would also like to thank my supervisor Prof. Risto Ilmoniemi, the head of the Department of Biomedical Engineering and Computational Science for his help during the later part of my graduate studies. I am grateful to Prof. (emer.) Toivo Katila for supervising the first part of my graduate studies, and especially for giving exceptionally instructive lectures on the theory of electromagnetism that have been really useful for my work.

My special thanks belong to Mr. Juha Hämäläinen, the acting managing director of Elekta Neuromag Oy, and to Mr. Stephen Otto, the chairman of the board of Elekta Neuromag Oy. They both have worked very hard to ensure that the collaboration between the company and the customers is as fluent and efficient as possible. This task is especially challenging in MEG where the developers of the technology and the users have a large variety of different backgrounds.

I am grateful to Ms. Riitta Pietilä, who, in addition to my closest scientific colleagues, has had the most important contribution to my thesis. Although coming from a different field, she has been extremely motivated to learn MEG and has helped me to present my work to interested non-mathematical audience. With her exceptionally strong attitude and unselfish character, she has always helped me with all kinds of preparations of my publications regardless of the large amount of work and tight schedules. I have always been able to count on her support and cooperation.

I would also like to thank all the colleagues that I have in Finland and abroad. Especially important for my thesis were the early infant studies where the main contributors were Prof. Toshiaki Imada, Prof. Marie Cheour, Prof. Patricia Kuhl, Dr. Elina Pihko, Prof. Yoshio Okada, and Dr. Leena Lauronen. Regarding the collaboration related to clinical applications of the methods presented here, I am especially grateful to Dr. Jyrki Mäkelä, Dr. Ritva Paetau, Dr. Michael Funke, and Dr. Eero Pekkonen. In addition to Low Temperature Laboratory, collaboration with the personnel of the BioMag laboratory of the Helsinki University Central Hospital has been especially important for me.

I am fortunate to have a very vast network of highly professional colleagues but the list of names is too long to be presented here. Of all those people I would especially like to mention Jukka Harju, Suvi Heikkilä, Juha Heiskala, Minna Huotilainen, Veikko Jousmäki, Jukka Knuutila, Atte Kojo, Jan Kujala, Petteri Laine, Matti Leiniö, Pantelis Lioumis, Burkhard Maess, Mordekhay Medvedovsky, Marjo Miettinen, Päivi Nevalainen, Jussi Nurminen, Riitta Salmelin, Johanna Salonen, Mika

Seppä, Tao Song, Antti Tarkiainen, Kimmo Uutela, Yoshio Yamada, and Candice Weir.

I want to thank all my friends for providing me with counterbalance, especially in the form of sports-related activities, to the demanding mental work. I am deeply grateful to my parents and my brother for their continuous support and encouragement throughout my thesis work.

Helsinki, September 2008

Samu Taulu

Contents

List of Publications

This thesis consists of an overview and of the following publications which are referred to in the text by their Roman numerals.

I Taulu S and Simola J. (2008). Multipole-based coordinate representation of a magnetic multichannel signal and its application in source modelling. Report TKK-F-A855.

II Taulu S and Kajola M. (2005). Presentation of electromagnetic multichannel data: The signal space separation method. J Appl Phys 97, 124905 1-10.

III Taulu S and Simola J. (2006). Spatiotemporal signal space separation method for rejecting nearby interference in MEG measurements. Phys Med Biol 51, 1759-1768.

IV Taulu S, Simola J, and Kajola M (2005). Applications of the Signal Space Separation Method. IEEE Trans Sign Proc 53, 3359-3372.

V Taulu S and Hari R. (2008). Removal of Magnetoencephalographic Artifacts With Temporal Signal-Space Separation: Demonstration With Single-Trial Auditory-Evoked Responses. Hum Brain Mapp, in press.

Author's contribution

I was the principal author in all papers I-V and performed all the simulations and data analysis. The other authors participated actively in planning of experiments and gave valuable ideas, comments and suggestions.

The most important basic theory of the thesis was developed in publication II together with the second author. Publication I connects this basic theory to a more general framework and demonstrates its usage in source modelling in addition to signal processing. The second author introduced useful ideas in publication I and participated in writing of the manuscript. I created the basic mathematical idea of publication III extending the theory of publication II, and the second author participated in the planning of the work and preparation of the manuscript. Publication IV was designed together with the other authors to demonstrate the applications based on the theory of publication II. In publication V, the second author suggested the experimental setup. I participated in the measurement and performed the subsequent signal processing and data analysis. The second author participated actively in planning and writing of publication V.

List of Abbreviations

DBS	Deep Brain Stimulator
DC	Direct Current
ECG	Electrocardiography
EEG	Electroencephalography
fMRI	Functional Magnetic Resonance Imaging
MRI	Magnetic Resonance Imaging
MCG	Magnetocardiography
MEG	Magnetoencephalography
MCE	Minimum Current Estimate
MNE	Minimum Norm Estimate
MSR	Magnetically Shielded Room
PET	Positron Emission Tomography
PCA	Principal Component Analysis
SSP	Signal Space Projection
SSS	Signal Space Separation
SNR	Signal-to-noise Ratio
SQUID	Superconducting Quantum Interference Device
SVD	Singular Value Decomposition
tSSS	Spatiotemporal Signal Space Separation
VNS	Vagal Nerve Stimulator
VSH	Vector Spherical Harmonic

1 Introduction

Multichannel measurement techniques are commonly used to record the spatial distribution of bio- and geomagnetic fields. An example of biomagnetic modalities is magnetoencephalography (MEG), which is investigated in this thesis.

Among the first multichannel measurements were geomagnetic observations recorded at numerous observatories that were distributed on the surface of the Earth. In the absence of electronics or hardware for data acquisition, the data analysis relied on sophisticated mathematical models describing the general nature of the geomagnetic field including contributions from the Earth and the outer space (Gauss and Weber, 1839; Garland, 1979). The geometry of modern MEG measurements (for a review, see Hämäläinen *et al.*, 1993) resembles that of the early geomagnetic recordings, but acquisition of MEG data includes a variety of digital signal processing methods and hardware solutions to ensure good data quality. Traditional problems of multichannel MEG, however, include the sometimes excessive external or nearby interference, spatial signal variations caused by moving head with respect to the sensors, and data visualization problems caused by the large number of sensors.

The initiative for the studies of this thesis arose from the infant MEG measurements conducted at the BioMag laboratory (HUSLAB, Helsinki University Central Hospital, Finland) (Cheour *et al.*, 2004; Imada *et al.*, 2006). Challenges caused by the strong interference fields compared to the tiny signals originating from the infant brain and the need to compensate for the different head positions and head movement encouraged the idea to develop a general-purpose signal processing method to alleviate these problems in as simple manner as possible.

The objective of the thesis is to show that it is feasible and advantageous to transform the multichannel MEG signals into a standardized and device-independent representation corresponding to the actual brain signals only, with the different kinds of distortions significantly suppressed. The transformation, enabled by the large amount of information in the multichannel measurement, is derived directly from the quasistatic Maxwell's equations with little additional assumptions. Interestingly, it turns out that the method resembles the approach taken by Gauss and Weber in their geomagnetism studies already in the early 19th century.

The most important applications arising from this theoretical idea are suppression of external interference, standardization of MEG signals with respect to the head position and sensor geometry, head movement compensation, removal of artifacts generated by sources in the proximity of the sensors, and facilitated source modelling utilizing the simplified representation of the data. All these applications exploit the same linear transformation of the multichannel MEG signals into a subspace with a lower dimension than the number of channels.

This overview of the thesis work is organized as follows. Chapter 2 describes the multichannel MEG measurements and their traditional challenges. Chapter 3 introduces the idea of representing the multichannel signal as a set of spatially independent coordinates. Chapter 4 shows that the signal space separation (SSS) method satisfies the general formalism of the coordinate representation of chapter 3. Finally, chapter 5 demonstrates the performance of SSS and its temporal extension (tSSS) in practical measurements and chapter 6 gives concluding remarks.

2 Magnetic multichannel measurements

2.1 Basic measurement geometry

This thesis considers multichannel measurements arranged as shown in Fig. 2.1. The purpose of such a measurement is to detect the magnetic field generated by the current distribution $\mathbf{J}_{\mathrm{in}}(\mathbf{r}')$. The electromagnetic signals are measured simultaneously with multiple sensors designed to receive as much information as possible of the current confined inside a certain volume, a sphere with radius r_{min} in this example. The object, possibly non-spherical, located inside the sphere enclosed by the sensors may be a human brain (MEG) or the Earth, for example.

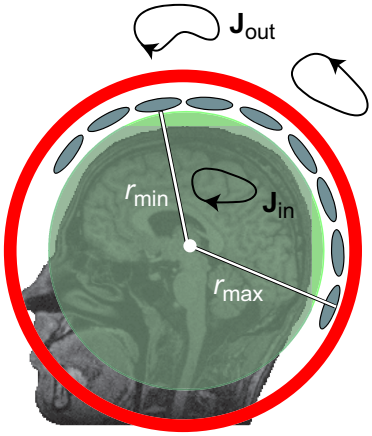

Figure 2.1: Schematic illustration of the basic geometry of a multichannel MEG measurement.

This work concentrates on the MEG method where the ultimate goal is the modelling and localization of the neurophysiological current sources based on the magnetic signals measured with submillisecond temporal resolution. This is called the inverse problem that does not have a unique solution (Helmholtz, 1853). By using suitable constraints, however, the brain activity can usually be estimated with good spatial accuracy, which makes MEG a valuable tool both in brain research and clinical neurological work (see, e.g., Hämäläinen *et al.*, 1993; Barth *et al.*, 1982; Paetau *et al.*, 1990; Mäkelä *et al.*, 2006).

It is evident from Fig. 2.1 that, if not properly taken into account, several imperfections may compromise the interpretation of the measured signals. First of all, the

signal distribution among the sensors depends on the relative position of the object of interest with respect to the sensors. The position may even be time-dependent. Furthermore, in addition to the interesting signal $\mathbf{J}_{\text{in}}(\mathbf{r}')$, external currents $\mathbf{J}_{\text{out}}(\mathbf{r}')$ are present in the environment and generate interference fields that are superimposed on the interesting fields and distort the result. For the purpose of source modelling, an ideal sampling of the field would yield uncorrelated pieces of information about $\mathbf{J}_{\text{in}}(\mathbf{r}')$. For technical reasons, however, this requirement is not fulfilled in the sensor outputs. It is impossible to arrange real sensors around the object without spatial redundancy in the information given by them.

This work presents a method that uniquely transforms the measured signals into device-independent components containing uncorrelated information about $\mathbf{J}_{\text{in}}(\mathbf{r}')$ with the contribution of $\mathbf{J}_{\text{out}}(\mathbf{r}')$ being suppressed. The method decomposes the measured signals into elementary fields obeying quasistatic Maxwell's equations and having measurable spatial frequencies. The internal and external currents correspond to separate elementary fields in this model. Essentially, the decomposition performs spatial filtering with the objective of bringing the measurement into accordance with Maxwell's equations with the interesting information packed as compactly as possible in a form free of imperfections.

2.2 Multichannel magnetoencephalography and its applications

The human brain is a network consisting of at least 10^{10} neurons on the cortex. The neurons are linked by about 10^{14} synapses forming a complex system capable of receiving, processing, and sending an immense amount of signals affecting the functioning of the whole human being. The information processing is based on small electric currents flowing in the neural network. Fig. 2.2 shows the propagation of a single action potential toward the synapse where it releases transmitter molecules producing a dipolar postsynaptic current and the associated magnetic field. When a large number of synapses act in concert this way, a magnetic field, large enough to be detected by the MEG sensors, arises. The detected field is mostly due to the net dipolar primary current produced at the synapses because the current corresponding to the action potential is quadrupolar and the associated field diminishes as a function of distance faster than the dipolar field.

MEG provides a non-invasive measurement of the electric activity in the brain's neural network. The excellent time resolution of MEG, better than 1 ms, enables practically real-time examination of brain functions. Similar temporal resolution is also achieved by electroencephalography (EEG), measurement of the voltage distribution on the scalp. The magnetic field, however, is less influenced by local differences in the conductivity distribution of the head, especially by the great difference between the conductances of the skull and the neural tissue. This renders MEG more useful than EEG in localization of the physiological current distribution.

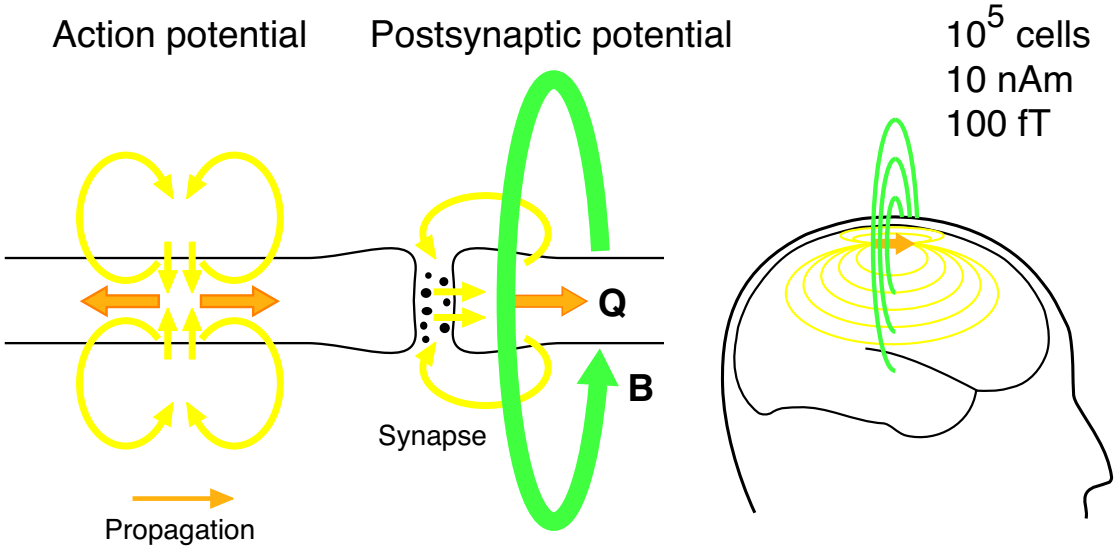

Figure 2.2: Postsynaptic current generating a magnetic field. The current is represented as a dipole moment with strength typically on the order of 10 nAm. This generates a magnetic field of about 100 fT at the distance of the MEG sensors.

The localization of the active brain areas based on the measured field requires the solution of the so called inverse problem. Solution of this problem is the ultimate goal of MEG recordings. In the source models, the current distribution is usually expressed as a sum of the primary and volume currents in the form $\mathbf{J} = \mathbf{J}^{\mathrm{p}} + \mathbf{J}^{\mathrm{v}}$, and the primary current distribution $\mathbf{J}^{\mathrm{p}}$ is estimated.

A unique solution of the inverse problem of MEG and EEG does not exist since any electromagnetic field can be produced by more than one current distribution inside a volume conductor (Helmholtz, 1853). Such current distributions are called equivalent in the following. By imposing suitable restrictions on the current distribution, one can often solve the inverse problem in a satisfactory way among a restricted set of allowed source models. The most common models are the single and multiple current dipoles (Brenner *et al.*, 1978; Tuomisto *et al.*, 1983; Scherg, 1990; Mosher *et al.*, 1992) and the minimum norm current estimates (Ioannides *et al.*, 1990; Dale and Sereno, 1993; Hämäläinen and Ilmoniemi, 1994; Pascual-Marqui *et al.*, 1994; Matsuura and Okabe, 1995; Uutela *et al.*, 1999). The current dipole model considers the primary current to be concentrated to a single point with a certain dipole moment. This model is especially simple in the case of a spherically symmetric conductor, where it can be shown that an equivalent source current is a triangle loop (Ilmoniemi, 1985; Ilmoniemi *et al.*, 1985) and the associated magnetic field outside the conductor has a simple analytic form (Sarvas, 1987). The spherically symmetric conductor model is sufficiently accurate in many cases, which has made Sarvas'

formula and localization of current dipoles very useful and popular in MEG. In contrast to current dipoles, the non-parametric models have the advantage of allowing for a more flexible set of solutions. The minimum norm current models, for example, seek for a current distribution having the smallest possible overall norm among the equivalent distributions of a given type. The minimization provides a possibly multi-focal current distribution estimate without extensive user intervention. This is advantageous especially in cases of complex source configurations.

All physical properties of electromagnetic fields are governed by Maxwell's equations. In neuromagnetism, most of the interesting phenomena occur at frequencies below 100 Hz allowing one to ignore the contribution of the time derivatives of the magnetic, $\mathbf{B}$, and electric, $\mathbf{E}$, fields (Plonsey and Heppner, 1967; Hämäläinen *et al.*, 1993). Thus, one arrives at the quasistatic Maxwell's equations:

$$\nabla \cdot \mathbf{E} = \rho/\epsilon_0, \tag{2.1}$$

$$\nabla \times \mathbf{E} = 0, \tag{2.2}$$

$$\nabla \cdot \mathbf{B} = 0, \tag{2.3}$$

$$\nabla \times \mathbf{B} = \mu_0 \mathbf{J}. \tag{2.4}$$

Here ρ is the charge density, ϵ_0 and μ_0 are the permittivity and permeability of vacuum, respectively, and $\mathbf{J}$ is the current density. All the forward and inverse models of MEG are based on these equations.

Applications of MEG

Among the functional brain mapping modalities including EEG, positron emission tomography (PET), and functional magnetic resonance imaging (fMRI), MEG has the best combination of excellent time and reasonable spatial resolution. Therefore, MEG has gained popularity in basic brain research and recently also in clinical studies.

Early MEG work concentrated especially on somatosensory and auditory processing. These brain functions are associated with quite focal and distinctive activation areas and were studied already in the 1970s (Brenner *et al.*, 1975, Teyler *et al.*, 1975, Hari *et al.*, 1980). With modern MEG devices covering the whole head more complicated studies examining higher brain functions and complex clinical conditions have become feasible (see, e.g., Hari *et al.*, 1993; Nishitani and Hari, 2002)

In addition to studies on brain activity evoked by certain stimuli, the spontaneous activity has been studied in detail. Especially, the rhythmic activity such as the α-(Williamson *et al.*, 1989) and μ-rhythm (Tiihonen *et al.*, 1989) has been investigated.

MEG has great potential in clinical work. For example, MEG is helpful in localization of functional areas in brain tissue suffering from distortions caused by a tumor. In such a case, the anatomical mapping by magnetic resonance imaging (MRI) or some other suitable modality gives information about the tumor but leaves uncertainty about the functional areas that should be preserved in surgery. Thus, MEG is a very valuable tool in presurgical mapping (Gallen *et al.*, 1993; Mäkelä *et al.*, 2006). Another major application area is localization of epileptic foci (Barth *et al.*, 1982; Paetau *et al.*, 1990; Shibasaki *et al.*, 2007). The method is very useful also in clinical research, like in studies on response mechanisms to deep brain stimulation (DBS) (Mäkelä *et al.*, 2007; Kringelbach *et al.*, 2007). Stimulation of the brain with DBS and with the vagal nerve stimulator (VNS) aims at alleviating the symptoms of Parkinson's disease and epilepsy (Rodriguez-Oroz *et al.*, 2005; George *et al.*, 2000). Thorough understanding on how the stimulation affects the brain is still lacking and MEG may be able to provide insight into the open questions.

The sensitivity of MEG measurements to different kinds of disturbances has been a significant obstacle in clinical examinations; the ambient interfering magnetic fields are six to eight orders of magnitude higher that the biomagnetic fields, see Fig. 2.3. Also, traditional signal processing methods have not been efficient enough to allow studies involving moving uncooperative patients or medical equipment causing strong magnetic interference, e.g., VNS or DBS. The work presented in this thesis aims at removing or at least alleviating these problems. These general problems specific to MEG will be discussed in more detail in section 2.5.

2.3 Measurement of MEG signals

The amplitude of a typical evoked brain field is on the order of 100 fT at a distance of a couple of centimeters from the surface of the head. In comparison, the static field of the Earth is about 10^8 times larger than this. The weakness of the brain signals creates a special challenge on the measurement instruments and external interference suppression methods. This section gives a brief introduction to the MEG instrumentation; the interference reduction methods will be dealt with in section 2.5.

Although the first MEG measurement by Cohen (Cohen, 1968) was carried out using a single induction coil, today the superconducting quantum interference device (SQUID) is considered the only practical sensor for MEG measurements. The SQUID (Zimmerman *et al.*, 1970; Cohen, 1972; Lounasmaa, 1974) is a superconducting loop interrupted by one or two Josephson junctions (Josephson, 1962). Owing to its superior noise performance the latter, called dc SQUID, is now solely used in MEG. With a suitable bias current being fed through the dc SQUID, the voltage across the SQUID is periodic as a function of the external magnetic field. In MEG, the SQUID is kept at a constant working point by a feedback current that is linearly

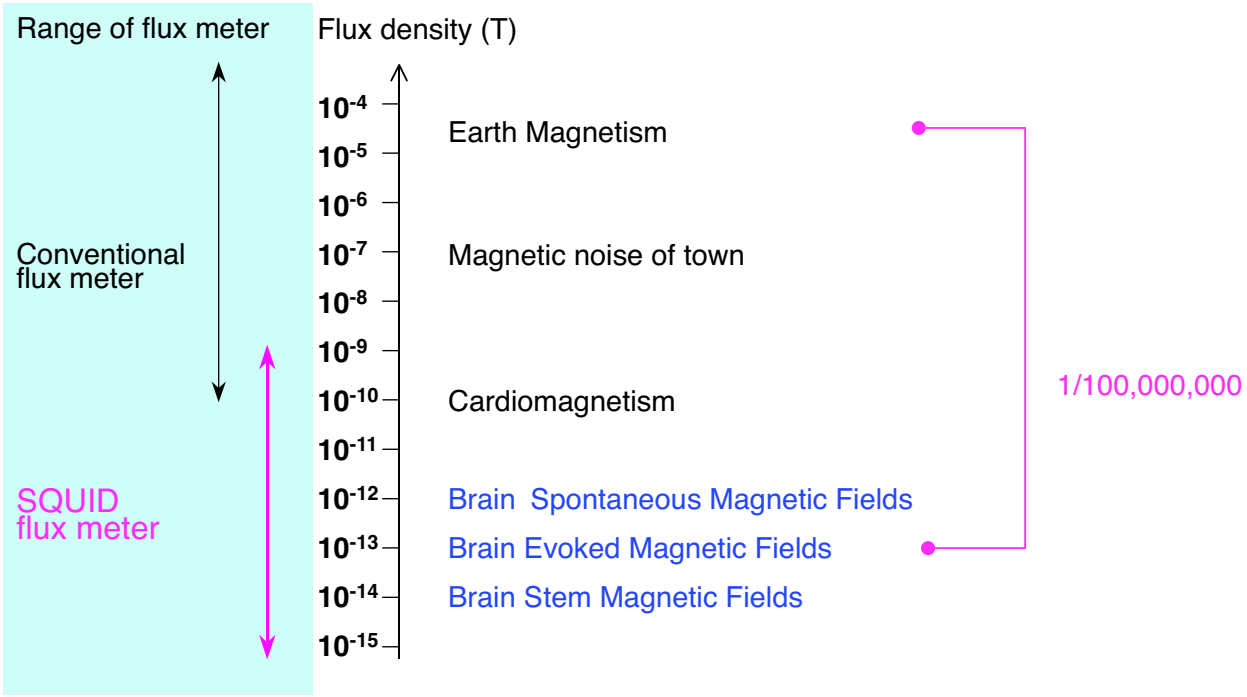

Figure 2.3: Amplitudes of some typical magnetic fields. The left panel shows the range of the conventional magnetic flux meter and the SQUID sensor.

proportional to the external magnetic field. Thus, the strength of the feedback gives a measure of the magnetic field (Ryhänen *et al.*, 1989).

The magnetic field is coupled to the SQUID through a flux transformer consisting of a pickup coil and an input coil, as shown if Fig. 2.4. The flux measured by the SQUID is a product of the current flowing in the flux transformer and the mutual inductance between the SQUID and the transformer. The pickup coils are usually arranged as magnetometers or gradiometers. The magnetometer is typically a single loop measuring the projection of the magnetic field to the normal of the magnetometer plane. The first order gradiometers consist of two identical loops wound in opposite directions. This configuration measures the planar or axial derivative of the field, which makes the gradiometers less sensitive to far-away interference sources than the magnetometers. On the other hand, the magnetometers couple better to fields generated by deep brain sources located closer to the center of the head and relatively far from the sensors.

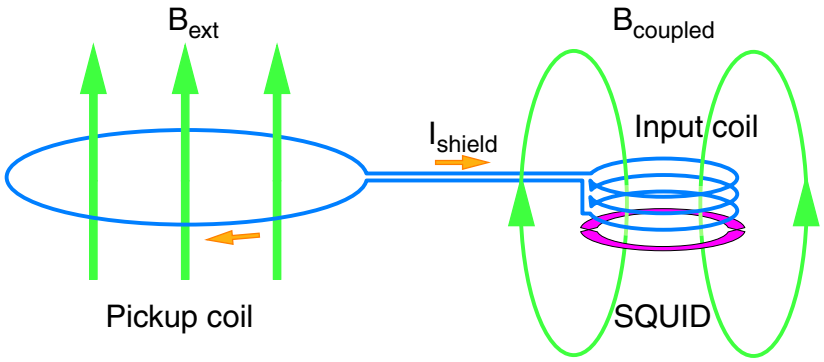

Figure 2.4: The principle of flux transforming. The field threading the pickup loop generates a shielding current providing the input flux of the SQUID through the input coil.

The first multichannel MEG devices in the 1980s had 4-7 channels covering an area ranging from only a few cm to about 10 cm in diameter (Ilmoniemi *et al.*, 1984; Romani *et al.*, 1985; Williamson *et al.*, 1985, Knuutila *et al.*, 1987). A substantial improvement in the coverage was achieved when devices having more than 20 channels emerged. For example, the number of channels of the devices manufactured at the Helsinki University of Technology and Neuromag Ltd. rose from 24 (Kajola *et al.*, 1989) to 122 (Ahonen *et al.*, 1992) between 1989 and 1992. Today, the state-of-the-art MEG devices contain more than 200 channels providing for a good whole-head coverage. Some of the major commercially available MEG systems

are Elekta Neuromag Oy's (Helsinki, Finland) 306-channel system employing magnetometers and planar gradiometers, the 248-channel system of 4D-Neuroimaging Ltd. (San Diego, USA) having magnetometers, and Yokogawa's (Tokyo, Japan) 160-channel system utilizing axial gradiometers. A number of 275-channel systems with axial gradiometer sensors produced by the former CTF/VSM (Port Coquitlam, Canada) company are still in use. These different devices are used in research institutes and in clinical laboratories. They are accompanied with the necessary electronics, workstations, software, and equipment for generating various sensory stimuli in different experiments.

The design of a multichannel MEG device contains several non-trivial decisions concerning especially the geometry of the sensor array, proper number of channels, and the configuration of the pickup loops. It is crucial to realize that the performance of the array has to be optimized by considering the information acquired simultaneously from all channels instead of separately optimizing individual channels. This is based on the fact that a multichannel MEG measurement can be considered as spatial sampling of the magnetic field. Thus, a thorough understanding of sampling theory is necessary in the development of MEG devices. The theory (Ahonen *et al.*, 1993) shows that the spatial frequencies of MEG signals are limited to a relatively low end of the spectrum. As a consequence, there is an upper limit to the practical number of sensors and a lower limit to the practical minimum distance between adjacent sensors. Despite being of fundamental nature in the design of multichannel sensor arrays, the sampling theory has not been very extensively used by other investigators. Some groups, however, have utilized a similar approach. For references, see, e.g., (Hochwald and Nehorai, 1997; Naddeo *et al.*, 2002).

The design of the 306-channel MEG system of Elekta Neuromag Oy is based on the concepts of sampling theory. The array consists of sensor elements each containing one magnetometer and two orthogonal planar gradiometers. This design guarantees that each sensor element provides three independent pieces of information as the current sensitivity patterns of these three pickup coils are orthogonal. Altogether 306 independent channels are obtained comprising of 510 loops since each of the 204 gradiometers consists of two loops and the 102 magnetometers have one loop. Information theoretical considerations based on Shannon's theory (Shannon, 1948; Shannon, 1949) have been used to evaluate this and the other existing MEG systems (Nenonen *et al.*, 2004).

In addition to having a good spatial coverage, the response of a modern multichannel MEG device must be consistent with Maxwell's equations. That is, the array must contain minimal manufacturing errors and all significant imperfections have to be quantitatively known in order to take them into account in data analysis. The raw MEG signals always contain some imperfections because of errors in calibration coefficients, knowledge about the sensor geometry, balance of the gradiometers, and cross-talk between the sensors. Bias is introduced if analysis models derived from Maxwell's equations assuming perfect measurement accuracy are used on data and

sensor information containing these distortions.

Other multichannel measurements

In addition to MEG, there are also other multichannel measurement modalities related to the schematic illustration of Fig. 2.1. Probably the first multichannel measurements were the geomagnetic observations made by different observatories around the world in the nineteenth century. Gauss and Weber (Gauss and Weber, 1839; Garland, 1979) developed a mathematical theory for the magnetic measurements by expressing the fields as expansions of harmonic functions. The theory first considered the signals to arise from currents flowing inside of the Earth and then discussed the possible contributions from the outer space on the measurements made on the surface of the Earth. It was concluded that the observations were dominated by fields arising from underground currents. Modern geomagnetic measurements consist of a large number of magnetic registrations made by observatories and satellites (see, e.g., Tank, 2000; Sabaka *et al.*, 2004; Lesur, 2006)

Today, numerous medical examinations utilize multichannel measurements. In modern magnetocardiography (MCG), the magnetic field produced by the heart is measured with multiple sensors outside of the torso (Nenonen and Katila, 1991; Nenonen *et al.*, 1991). Electroencephalography (EEG) measures differences in the electric potential on the surface of the head with multiple electrodes. It differs from Fig. 2.1 in the sense that in EEG, the sensors are attached to the head and therefore head movements do not modulate the measured signal. The counterpart of EEG in examinations of the heart is electrocardiography (ECG).

A recent theory suggests that earthquakes may be preceded by geomagnetic changes caused by mechanical deformation of rocks, (see, e.g., Fujinava and Takahashi, 1998; Rabinovitch *et al.*, 2007). Multichannel measurements of the associated magnetic fields could enable a method to forecast the onset of a quake, but this approach has also been criticized (Geller, 1997).

2.4 Mathematical representation of MEG signals

The signal recorded by the jth sensor is proportional to the flux

$$\phi_j = \int_{S_j} \mathbf{B}(\mathbf{r}) \cdot d\mathbf{S}, \tag{2.5}$$

where S_j indicates the area confined by the pickup coil. In forward calculations of the sensor signals, one has to approximate the surface integral numerically in the

form

$$\phi_{\mathrm{FC},j} = \int_{S_j} \mathbf{B}_{\mathrm{FC}}(\mathbf{r}) \cdot d\mathbf{S} \approx \sum_{p=1}^{M} \mathbf{B}_{\mathrm{FC}}(\mathbf{r}_p) \cdot \Delta\mathbf{S}_p, \tag{2.6}$$

where the subscript FC stands for forward calculation based on some source model and the integration points $\mathbf{r}_p$ are chosen to approximate the surface integral with adequate precision. The accuracy increases as a function of the number of integration points, M, and thus there is a trade-off between accuracy of the model and computational efficiency. Numerical surface integral estimates with different accuracies can be found, e.g., in (Abramowitz and Stegun, 1964). Typically, M ranges from 4 to 16.

According to Fig. 2.1, the brain and external interference sources contribute to the field in the form $\mathbf{B}(\mathbf{r}) = \mathbf{B}_{\mathrm{in}}(\mathbf{r}) + \mathbf{B}_{\mathrm{out}}(\mathbf{r})$ leading to signal

$$\phi_j = \int_{S_j} [\mathbf{B}_{\mathrm{in}}(\mathbf{r}) + \mathbf{B}_{\mathrm{out}}(\mathbf{r})] \cdot d\mathbf{S} \equiv \phi_{\mathrm{in},j} + \phi_{\mathrm{out},j}. \tag{2.7}$$

In some cases there may exist sources of field also in the intermediate volume between the green sphere and the red circle in Fig. 2.1. Then, in the sense of the previous equation, the signal is of the form

$$\phi_j = \phi_{\mathrm{in},j} + \phi_{\mathrm{out},j} + \phi_{\mathrm{inter},j}. \tag{2.8}$$

A common model for the signal produced by biomagnetic sources is the lead field representation (Malmivuo, 1976; Tripp, 1983), where the signal is represented as a projection of the current to the lead field $\mathbf{L}_j$ of the particular sensor. In mathematical terms

$$\phi_{\mathrm{in},j} = \int_{v'} \mathbf{L}_j(T, \mathbf{r}') \cdot \mathbf{J}_{\mathrm{in}}(\mathbf{r}')dv' = \int_{v'} \mathbf{L}_j^{\mathrm{p}}(T, \mathbf{r}') \cdot \mathbf{J}_{\mathrm{in}}^{\mathrm{p}}(\mathbf{r}')dv' \tag{2.9}$$

where T is an operator transforming the sensor geometry into the coordinate system of the head and $\mathbf{L}_j^{\mathrm{p}}$ is the lead field corresponding to primary current. Consequently, given a current distribution $\mathbf{J}_{\mathrm{in}}(\mathbf{r}')$, the sensor output depends on the position and orientation of the head with respect to the sensor.

Usually the lead field is defined for the primary current. If the magnetic field of a current dipole $\mathbf{Q}$ at an arbitrary position $\mathbf{r}_{\mathrm{q}}$ can be calculated, the lead field is obtained from the relation

$$\phi_{\mathrm{in},j} = \mathbf{L}_j^{\mathrm{p}}(T, \mathbf{r}_{\mathrm{q}}) \cdot \mathbf{Q}. \tag{2.10}$$

This lead-field formulation requires knowledge of the conductivity distribution in order to take the volume currents properly into account.

The lead fields of individual sensors generally overlap, that is, with $j \neq k$

$$\int_{v'} \mathbf{L}_j \cdot \mathbf{L}_k dv' \neq 0 \tag{2.11}$$

and

$$\int_{v'} \mathbf{L}_j^{\mathrm{p}} \cdot \mathbf{L}_k^{\mathrm{p}} dv' \neq 0 \tag{2.12}$$

For illustration, Fig. 2.5 shows the lead fields $\mathbf{L}^{\mathrm{p}}$ of planar gradiometers and magnetometers of the Elekta Neuromag's 306-channel device. The orthogonality of the lead fields of the three sensors on a single sensor element is easily visualized. It is technically not feasible, however, to create a sensor array with orthogonal lead fields between all sensors.

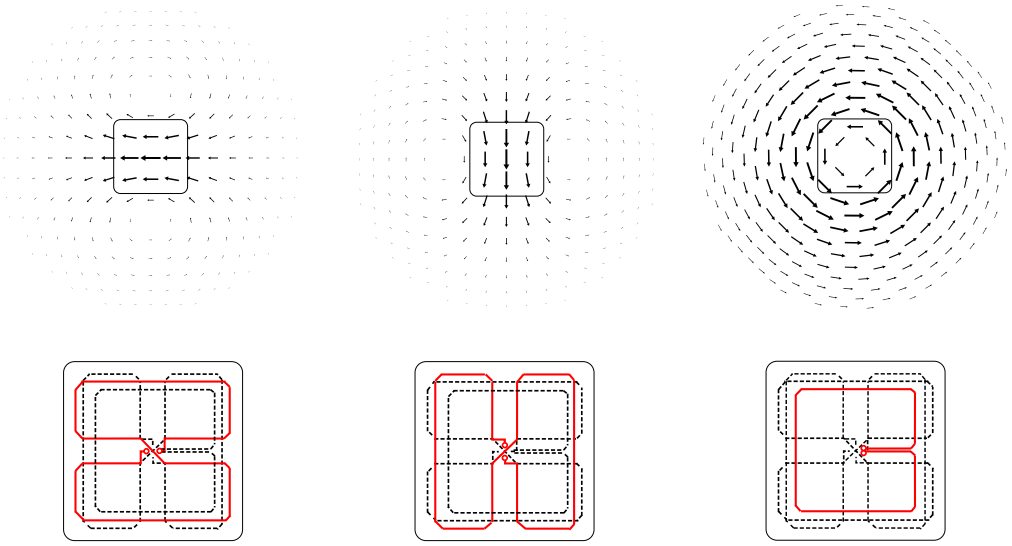

Figure 2.5: Lead fields of two orthogonal gradiometers and a magnetometer.

Let us now define the signal vector ϕ as consisting of the signal values of the N individual sensors:

$$\phi = [\phi_1 \ \phi_2 \ \ldots \ \phi_N]^{\mathrm{T}}, \tag{2.13}$$

where T denotes transpose. The vector ϕ could be a sample of raw data at time instant t, averaged response, or contain spectral information from different channels. Based on equations 2.7 and 2.9, the signal vector is more specifically expressed as

$$\phi(\mathbf{J}_{\mathrm{in}}, \mathbf{J}_{\mathrm{out}}, T) = \phi_{\mathrm{in}}(\mathbf{J}_{\mathrm{in}}, T) + \phi_{\mathrm{out}}(\mathbf{J}_{\mathrm{out}}) \tag{2.14}$$

The N-dimensional vectors ϕ define the signal space of MEG. This highly useful concept was introduced to MEG signal analysis in the 1980s (Ilmoniemi, 1981; Ilmoniemi and Williamson, 1987; Ilmoniemi *et al.*, 1987).

2.5 Basic problems of MEG measurements

External interference

Fig. 2.3 shows typical variations of amplitudes of different kinds of fields present in an unshielded environment. The fields generated by the brain are several orders of magnitude smaller than most of the fields considered interference in MEG. Because of this huge amplitude difference, the MEG measurements are usually carried out in magnetically shielded rooms (MSR) (Cohen, 1970; Kelhä *et al.*, 1982, Bork *et al.*, 2001). The shielding is based on the wall structure of the MSR that typically utilizes aluminium and high permeability ferromagnetic alloy composed of iron and nickel, often called μ-metal. In the low frequency range the shielding is based on the ferromagnetic μ-metal whereas in the high frequency end the shielding effect is dominated by eddy currents in the aluminium.

To clarify the performance of passive shielding with MSR, let us now divide the volume of external interference sources into volumes ρ and $\mathbf{R}$ located inside and outside of the MSR, respectively. Both of these volumes are external to the sensor array in the sense of Fig. 2.1. The passive shielding only suppresses interference arising from the large volume $\mathbf{R}$, and so the original interference

$$\phi_{\mathrm{out}}(\mathbf{J}_{\mathrm{out}}) = \phi_{\mathrm{out}}[\mathbf{J}_{\mathrm{out}}(\rho)] + \phi_{\mathrm{out}}[\mathbf{J}_{\mathrm{out}}(\mathbf{R})] \tag{2.15}$$

has the following residual after introduction of the magnetic shield:

$$\phi_{\mathrm{r,out}}(\mathbf{J}_{\mathrm{out}}) = \phi_{\mathrm{out}}[\mathbf{J}_{\mathrm{out}}(\rho)] + \phi_{\mathrm{r,out}}[\mathbf{J}_{\mathrm{out}}(\mathbf{R})] \tag{2.16}$$

with typically the attenuation $||\phi_{\mathrm{r,out}}[\mathbf{J}_{\mathrm{out}}(\mathbf{R})]||/||\phi_{\mathrm{out}}[\mathbf{J}_{\mathrm{out}}(\mathbf{R})]|| << 1$. With the modern design, attenuation factors of 35 dB and 45 dB have been reached for rooms with the μ-metal in a single or two separate shells, respectively, at a frequency of 0.1 Hz. A heavy room with eight layers has been reported to have an attenuation of more than 100 dB (Bork *et al.*, 2001).

The residual $\phi_{\mathrm{r,out}}(\mathbf{J}_{\mathrm{out}})$ may severely interfere with the brain signals, especially in the presence of interference sources inside the MSR producing signals that are not attenuated by the passive shielding. In order to suppress the residual interference, several methods have been developed. The most common of them are the reference sensor method (see, e.g., Vrba and Robinson, 2001), and projection methods, especially the signal space projection (SSP) (Uusitalo and Ilmoniemi, 1997).

Conventional reference sensors are located sufficiently far away, typically more than 10 cm, from the brain so that they can be assumed to record interference only. Then the interference field is parametrized by, e.g., a low-order Taylor expansion whose coefficients can be estimated from the signals of the reference sensors. A fundamental problem with the reference sensors is that the interference field is recorded quite far

away from the proper sensors. The harmful signal distortion takes place at the sites of the proper sensors and so the interference components estimated from the reference sensors have to be extrapolated over a long distance making the method prone to errors in the geometry and calibration of the sensor arrangement. In addition, nearby interference sources, such as vagal nerve stimulators (VNS) or braces, producing spatially complex fields cannot be effectively suppressed by the reference sensors. The traditional approach utilizing Taylor series converging at the origin is not even in theory applicable for attenuation of this nearby interference because the method assumes that all interference sources are further away than any of the MEG sensors.

The SSP method in its usual implementation is based on a statistical analysis on data measured with the proper sensors and containing typical interference patterns to be removed. By using, e.g., the principal component analysis (PCA), one can determine the subspace $\mathbf{U}$ of the signal space that contains the interference directions. Then the projection operator $\mathbf{P}_\perp = \mathbf{I} - \mathbf{U}\mathbf{U}^{\mathrm{T}}$ projects out the external interference:

$$\mathbf{P}_\perp \phi = \mathbf{P}_\perp(\phi_{\mathrm{in}} + \phi_{\mathrm{out}}) = \mathbf{P}_\perp \phi_{\mathrm{in}}. \tag{2.17}$$

SSP has the advantage that the interference is measured at the very site where it needs to be removed. In addition, calibration errors do not affect the performance of the method. A drawback is shown by Eq. (2.17), which indicates that removal of the interference by SSP generally distorts the brain signal as the projection operator $\mathbf{P}_\perp$ is not orthogonal to ϕ_{in}. This distortion can, however, be taken into account in source modelling by applying the projection operator also to the forward model. Because $||\mathbf{P}_\perp \phi_{\mathrm{in}}|| \leq ||\phi_{\mathrm{in}}||$, the amplitude of the brain signals may also decrease but for most practical cases this effect is quite insignificant. Another difficulty arises when the interference field changes significantly with time. Usually the SSP operator is calculated from an empty room measurement with no subject but only the interference sources present. Spatial patterns of typical environmental interference fields are usually stationary, whereas spatially and temporally complex interference, e.g., from stimulators attached to the body of a patient, may be difficult to suppress with SSP. The projection operator can, of course, be determined from the actual data but with complex interference this procedure is more difficult than with empty room interference. In such a situation, the interference is typically spread into a larger number of PCA components than the environmental empty room signal.

Head movements

A characteristic problem in MEG is related to the fact that the sensors are not attached to the head. Different locations of the subject with respect to the device hamper the comparison of data from different measurement sessions. Even more severe problems arise if the subject moves the head during the measurement, which may cause considerable source localization bias if the movement is not compensated

for. Head movements are unavoidable in many cases, e.g., with small children and some patient groups.

Assuming that the external interference has been removed from the measurement, the remaining signal is, according to Eq. (2.14), of the form $\phi_{\text{in}}(\mathbf{J}_{\text{in}}, T(t))$. The residual imperfection is the time-dependent transformation $T(t)$ between the head and the measurement device. In order to compensate for the head position differences, the data have to be transformed into a device-independent model that can be used for calculation of the virtual signals corresponding to a standard head position. Suitable models are, e.g., minimum norm and minimum current estimates (MNE and MCE) (Numminen *et al.*, 1995; Uutela *et al.*, 2001) and multipole expansion (Burghoff *et al.*, 2000). For movement compensation, the head position has to be tracked continuously or at least intermittently. This can be accomplished by attaching small magnetic coils to known locations on the head and activating them with signals having individual temporal patterns (Uutela *et al.*, 2001). Amplitudes corresponding to individual coils can be extracted and the head position with respect to the device can be calculated from the amplitude information.

Source modelling

Once the transformation $T(t)$ is known, the signal $\phi_{\text{in}}(\mathbf{J}_{\text{in}}, T(t))$ can be used for source modelling. One can, for example, fit a specific model to the data by adjusting the model parameters to minimize the difference between $\phi_{\text{in}}(\mathbf{J}_{\text{in}}, T(t))$ and the forward model of Eq. (2.6). Another possibility is to use the non-parametric models such as MCE, where the L1 norm of the current distribution is minimized over the source surface or volume. If the number of channels and integration points are N and M, respectively, the forward model requires NM calculations, which is computationally quite intensive when the number of channels is large and a high accuracy is needed for the numerical surface integral of Eq. (2.6). Furthermore, due to the overlapping lead fields of the sensors, the Gram matrix containing inner products of the lead fields, shown by Eq. (2.12) and employed by MNE and MCE, is ill-posed and has to be regularized. The regularization is case-sensitive and often requires user intervention without quantitative criteria. For a review of numerical regularization methods, see (Hansen, 2006).

General signal processing in MEG

Traditional preprocessing methods of MEG data have been mostly tailored to handle one imperfection at a time. This has led to a chain of operations and sometimes unnecessarily complicated processing. For example, in the case of a moving subject one would first suppresses the contribution of external interference, then compensate for the movement by MNE, and finally perform source modelling on $\phi_{\text{in}}(\mathbf{J}_{\text{in}}, T(t))$

requiring a large number of forward calculations and possibly numerical regularization.

Specifically, some cases with nearby interference sources have been too difficult for existing preprocessing methods. For example, the quality of MEG data from pediatric epilepsy patients is significantly deteriorated in more than 50 % of the cases, often due to nearby artifact sources and therapeutic hardware such as VNS devices (Paetau, 2008).

Every MEG measurement contains the brain signals in an undistorted form. Distortion caused by external interference or changing head position does not destroy the brain signal as long as the sensors are operational. In order to recover the true brain signals, the imperfections have to be recognized and their contribution removed from the data. Chapter 3 introduces the basic idea of utilizing the generous oversampling of modern MEG devices to achieve this goal.

3 Coordinate representation of multichannel signals

3.1 Sampling of the magnetic field

This section is entirely based on publication I. The output of a multichannel measurement can be formulated as a mapping from current to output $F[\mathbf{J}_{\mathrm{in}}(\mathbf{r}', T(t)) + \mathbf{J}_{\mathrm{out}}(\mathbf{r}')]$, which indicates that the contribution of the brain and interference currents is measured with a device whose signal also depends on the transformation $T(t)$ that relates the sensor geometry with the coordinate system of the head. This formulation describes the apparent problems of MEG to a large extent.

As an ultimate preprocessing method, we search for a transformation $F \rightarrow f$, where $f[\mathbf{J}_{\mathrm{in}}(\mathbf{r}')]$ maps the brain sources into device-independent components with the contribution of $\mathbf{J}_{\mathrm{out}}(\mathbf{r}')$ and $T(t)$ eliminated. Furthermore, we prefer f to be a mapping from the N-dimensional signal vector into an n-dimensional vector of uncorrelated point-like virtual sensors with $n < N$.

The transformation f should only change the representation of the data into a more favourable form without loosing information about $\mathbf{J}_{\mathrm{in}}(\mathbf{r}')$. Such a request can only be satisfied if the measured signal can be uniquely parametrized with the number of parameters being smaller than N, the number of sensors. That is, N must exceed m, the number of degrees of freedom of the neuromagnetic field that can be measured with the multichannel device.

Any source distribution can be expressed as a superposition of elementary currents. In the case of physiological currents inside a volume conductor, a current dipole can be chosen as an elementary current. In general, one current dipole has six degrees of freedom describing the three-dimensional location and orientation of the dipole. Thus, a current distribution consisting of n_{d} dipoles would generate a magnetic field with $6n_{\mathrm{d}}$ degrees of freedom. As no upper limit for n_{d} can be assumed, the MEG signal apparently seems to have an infinite number of degrees of freedom.

The sampling theory of neuromagnetic fields (Ahonen *et al.*, 1993) shows, however, that in MEG signals, the contribution of spatial frequencies higher than $(2d)^{-1}$ is below the sensor noise and therefore insignificant when d is the shortest distance between a source of magnetic field and a MEG sensor. In other words, the part containing biomagnetic information in the measured signals is limited in spatial complexity. This gives us the general idea of treating the MEG signals in the same way as the Fourier transform treats digitized temporal signals having limited frequency contents. The transformation $F \rightarrow f$ could be, for example, a decomposition of the spatially sampled MEG signals to a set of Fourier-like spatial basis components.

3.2 General coordinate representation of a multichannel measurement

A discrete signal $\mathbf{s} = [s_0\ s_1\ \ldots\ s_{(N_\mathrm{s}-1)}]^\mathrm{T}$, with T indicating transpose and N_s being the number of samples, containing a finite number of degrees of freedom is conveniently expressed as an expansion of discrete basis components:

$$\mathbf{s} = \sum_{k=0}^{N_\mathrm{s}-1} c_k \mathbf{f}_k, \tag{3.1}$$

where the vectors $\mathbf{f}_k$ are the basis vectors and the coefficients c_k are the coordinates of $\mathbf{s}$ in this basis. In the matrix form, we have

$$\mathbf{s} = \mathbf{F}\mathbf{c}, \tag{3.2}$$

where $\mathbf{F} = [\mathbf{f}_0\ \mathbf{f}_1\ \ldots\ \mathbf{f}_{N_\mathrm{s}-1}]$ is the signal basis and $\mathbf{c} = [c_0\ c_1\ \ldots\ c_{N_\mathrm{s}-1}]^\mathrm{T}$ contains the coordinates of $\mathbf{s}$ in this basis. Specifically, in Fourier transform, the basis $\mathbf{F}$ consists of the sine and cosine components up to the Nyquist frequency (Nyquist, 1928) and the coordinates $\mathbf{c}$ are the Fourier coefficients. They contain all the information conveyed by the discretized signal $\mathbf{s}$. According to Eq. (3.2), the coefficients can be decomposed as

$$\mathbf{c} = \mathbf{F}^\dagger \mathbf{s}, \tag{3.3}$$

where $\mathbf{F}^\dagger = (\mathbf{F}^\mathrm{T}\mathbf{F})^{-1}\mathbf{F}^\mathrm{T}$ is the pseudoinverse of $\mathbf{F}$. In the Fourier transform, the sampled data segment is usually chosen in such a way that the basis vectors are linear algebrally orthogonal over the sampled time interval. Then, $\mathbf{F}^\mathrm{T}\mathbf{F}$ is a diagonal matrix.

The signal vector ϕ of an MEG measurement is also a discretized signal but now the samples are produced by spatial instead of temporal sampling. According to the sampling theory mentioned before (Ahonen *et al.*, 1993), a modern multichannel MEG array provides an adequately sampled signal vector ϕ in Nyquist's sense. In order to create a representation similar to Eq. (3.2) for the MEG signals, we first expand the magnetic field with vector-valued basis functions $\mathbf{b}_k$:

$$\mathbf{B}(\mathbf{r}) = \sum_{k=1}^{m} x_k \mathbf{b}_k(\mathbf{r}) + \mathbf{R}(\mathbf{r}, m), \tag{3.4}$$

where the truncation order m is chosen in such a way that the residual $\mathbf{R}(\mathbf{r}, m)$ is below the instrument noise. As in Fourier-series, the coefficients x_k are the strengths or amplitudes of the basis functions $\mathbf{b}_k(\mathbf{r})$, given $\mathbf{B}(\mathbf{r})$, that should cover all measurable degrees of freedom. That is, they should correspond to the spatial frequencies present in the biomagnetic part of the MEG signal. Each of the basis functions corresponds to a basis vector ϕ_k with its jth component being the flux through the jth pickup loop:

$$\phi_{kj} = \int_{S_j} \mathbf{b}_k(\mathbf{r}) \cdot d\mathbf{S} \tag{3.5}$$

Thus, with the residual $\mathbf{R}(\mathbf{r}, m)$ omitted, Eq. (3.4) transforms to

$$\phi = \sum_{k=1}^{m} x_k \phi_k \equiv \Phi \mathbf{x} \tag{3.6}$$

which defines the basis

$$\Phi = [\phi_1 \ \phi_2 \ \ldots \ \phi_m] \tag{3.7}$$

and the coordinates of a multichannel MEG measurement

$$\mathbf{x} = [x_1 \ x_2 \ \ldots \ x_m]^{\mathrm{T}}. \tag{3.8}$$

The coordinates can be estimated as

$$\hat{\mathbf{x}} = \Phi^{\dagger} \phi. \tag{3.9}$$

3.3 Unique device-independent coordinates of MEG signals

Visualization of higher than three-dimensional signal bases is extremely difficult without abstract mathematical concepts. Therefore, it is illustrative to start by investigating the simple Cartesian coordinates of a given location $\mathbf{r}$. In comparison to the lead field form of 2.9, the Cartesian coordinates can be expressed as inner products $x = \mathbf{e}_{\mathrm{x}} \cdot \mathbf{r}$, $y = \mathbf{e}_{\mathrm{y}} \cdot \mathbf{r}$, and $z = \mathbf{e}_{\mathrm{z}} \cdot \mathbf{r}$, where $\mathbf{e}_{\mathrm{x}}$, $\mathbf{e}_{\mathrm{y}}$, and $\mathbf{e}_{\mathrm{z}}$ are the orthogonal x-, y-, and z-directional unit vectors. Thus, the Cartesian coordinates can be regarded as virtual channels containing orthogonal information and together leaving no ambiguity about the location of the interesting object.

In biomagnetism, we seek a transformation $F \rightarrow f$ such that f would consist of the coordinates $\mathbf{x}$ revealing the exact current distribution. Due to the non-uniqueness of the electromagnetic inverse problem (Helmholtz, 1853), however, such a goal cannot be achieved. If no a priori assumptions other than the division shown in Fig. 2.1 are made, the achievable coordinates would ideally represent spatially uncorrelated features of the general current distribution. Specifically, we would like to have the contributions of $\mathbf{J}_{\mathrm{in}}$ and $\mathbf{J}_{\mathrm{out}}$ separated as $\mathbf{x} = [\mathbf{x}_{\mathrm{in}}^{\mathrm{T}} \ \mathbf{x}_{\mathrm{out}}^{\mathrm{T}}]^{\mathrm{T}}$ satisfying

$$x_{\mathrm{in},j} = < \lambda_j, \mathbf{J}_{\mathrm{in}} > \tag{3.10}$$

and

$$< \lambda_j, \lambda_k > = \delta_{jk}, \tag{3.11}$$

where $< \cdot >$ indicates inner product, λ_j is the lead field corresponding to the j:th coordinate, and δ_{jk} is Kronecker's delta function.

This formulation is consistent with the non-uniqueness of the magnetic inverse problem if there exists a non-zero current $\mathbf{J}_{\perp}$ that satisfies $< \lambda_j, \mathbf{J}_{\perp} >= 0$ for every j.

Current distributions $\mathbf{J}_{\text{in}}$ and $\mathbf{J}_{\text{in}}+\mathbf{J}_{\perp}$ would then both produce the same coordinates $\mathbf{x}_{\text{in}}$.

In practice, to achieve such a coordinate representation, the basis Φ must contain all relevant spatial frequencies. Furthermore, the geometry of the sensor array with respect to the head must be taken into account in the calculation of Φ in order to get device-independent coordinates. The next chapter shows how these requests can be fulfilled and the contributions of $\mathbf{J}_{\text{in}}$ and $\mathbf{J}_{\text{out}}$ separated into their own sets of coordinates.

4 The signal space separation method (SSS)

4.1 Harmonic basis functions

In the subsequent sections, a spatial basis is derived for MEG that, in comparison to SSP for example, does not involve any statistics. The idea is to create a basis allowing for the device-independent representation of the data that is capable of significantly suppressing the contribution of the distortions typical to MEG.

Vector-valued basis functions are needed to achieve a coordinate representation of a biomagnetic multichannel measurement, as stated by Eq. (3.4). Maxwell's equations cover all properties of the magnetic field, so let us start from the quasistatic Maxwell's equations Eq. (2.3) and Eq. (2.4). These equations can be linked to the geometry of a MEG measurement shown in Fig. 2.1

In chapter III of publication II, the suitable basis functions are derived starting from the fact that every sensor is located in a current-free volume reducing Eq. (2.4) to

$$\nabla \times \mathbf{B} = 0. \tag{4.1}$$

Consequently, the magnetic field can be expressed as the gradient of a harmonic scalar potential V:

$$\mathbf{B} = -\mu_0 \nabla V, \tag{4.2}$$

where, due to relation $\nabla \cdot \mathbf{B} = 0$, V satisfies Laplace's equation

$$\nabla^2 V = 0. \tag{4.3}$$

In the spherical coordinate system (r, θ, φ), Laplace's equation has the series-form solution (e.g. Jackson, 1999) at field point $\mathbf{r}$

$$V(\mathbf{r}) = \sum_{l=0}^{\infty} \sum_{m=-l}^{l} \alpha_{lm} \frac{Y_{lm}(\theta, \varphi)}{r^{l+1}} + \sum_{l=0}^{\infty} \sum_{m=-l}^{l} \beta_{lm} r^l Y_{lm}(\theta, \varphi), \tag{4.4}$$

where Y_{lm} is the normalized spherical harmonic function and the coefficients α_{lm} and β_{lm} are called multipole moments. This expansion compactly represents the contribution of all sources generating a magnetic field. The two different parts of the expansion having different r-dependencies cover the convergence and divergence requirements of the fields produced by sources in different volumes of the space. The signal of a source in the volume containing the origin ($r' < r_{\text{min}}$) must be non-singular when $r' > r_{\text{min}}$. Similarly, the signal generated in the outside volume ($r' > r_{\text{max}}$) must be non-singular when $r' < r_{\text{max}}$. Consequently, the first sum in Eq. (4.4) describes fields generated by sources with $r' < r_{\text{min}}$ and similarly the second sum is related to sources with $r' > r_{\text{max}}$. As can be seen from Fig. 2.1, by

selecting the expansion origin in a suitable way, typically at the center of the volume enclosed by the sensor array, the contributions of the brain and interference sources are separated to the first and second sum of the expansion, respectively. At this point we assume that there are no sources in the volume defined by $r_{\mathrm{min}} < r' < r_{\mathrm{max}}$.

Publication II further showed that by inserting Eq. (4.4) into Eq. (4.2), the following expansion is obtained for the magnetic field:

$$\mathbf{B}(\mathbf{r}) = -\mu_0 \sum_{l=1}^{\infty} \sum_{m=-l}^{l} \alpha_{lm} \frac{\nu_{lm}(\theta,\varphi)}{r^{l+2}} - \mu_0 \sum_{l=1}^{\infty} \sum_{m=-l}^{l} \beta_{lm} r^l \omega_{lm}(\theta,\varphi), \qquad (4.5)$$

where $\nu_{lm}(\theta,\varphi) = \sqrt{(l+1)(2l+1)}\mathbf{V}_{lm}(\theta,\varphi)$ and $\omega_{lm}(\theta,\varphi) = \sqrt{l(2l+1)}\mathbf{W}_{lm}(\theta,\varphi)$ with $\mathbf{V}$ and $\mathbf{W}$ being the vector spherical harmonic functions defined by Hill (Hill, 1954; Arfken, 1985). Here the monopole term ($l = 0$) must be left out due to relation $\nabla \cdot \mathbf{B} = 0$ valid everywhere. An alternative way to formulate an expansion for $\mathbf{B}$ is to use recursive formulas for the derivatives of the harmonic scalar potential (Nolte *et al.*, 2001).

The question remains whether the residual in Eq. (3.4) is insignificant when truncating the series. This was investigated theoretically in publication II and experimentally in publication IV. The series was found to converge fast enough so that in typical MEG measurements, truncation of the two expansions in Eq. (4.5) at $l = L_{\mathrm{in}} = 8$ and $l = L_{\mathrm{out}} = 3$ was sufficient to ensure a negligible residual. Even in the case of 100 simultaneous current dipoles, $L_{\mathrm{in}} = 8$ is enough to reconstruct the brain signal with insignificant residual compared to sensor noise.

The relatively low expansion orders are sufficient because of the quite large distance between the sensors and sources of magnetic field, which applies to both the interesting and interfering sources. Because the series representing the neural sources converges fast as a function of distance, fields with the highest spatial frequencies corresponding to high l are attenuated below sensor noise at the distance of the sensors when the sensor noise level of the present SQUID technology, about 3 fT/$\sqrt{\mathrm{Hz}}$, is assumed. With $L_{\mathrm{in}} = 8$, the highest spatial frequencies are $9/(2\pi R)$ on a sphere with radius R. By setting the expansion origin approximately at the center of the brain, the closest sensors are typically at a distance of at least 10 cm from the origin. The corresponding highest spatial frequencies explained by our basis functions are then about 14.3 1/m. This is in agreement with the sampling theory (Ahonen *et al.*, 1993) stating that spatial frequencies higher than $(2D)^{-1} \approx 14.7$ 1/m are insignificant in MEG. Here, value $D = 34$ mm was used as the distance between adjacent sensors.

4.2 The SSS basis

The basis vectors corresponding to the VSH functions are calculated by Eq. (3.5) giving us vectors $\mathbf{a}_{lm}$ and $\mathbf{b}_{lm}$ corresponding to the basis functions $-\mu_0 r^{-(l+2)}\nu_{lm}$ and $-\mu_0 r^l \omega_{lm}$, respectively. Thus, our linear model for any momentary signal vector ϕ, based on Eq. (3.6) - Eq. (3.8), is

$$\phi = \mathbf{S}\mathbf{x}, \tag{4.6}$$

where the SSS basis $\mathbf{S} = [\mathbf{S}_{\text{in}}\ \mathbf{S}_{\text{out}}]$ separates the contribution of $\mathbf{J}_{\text{in}}$ and $\mathbf{J}_{\text{out}}$ as

$$\mathbf{S}_{\text{in}} = [\mathbf{a}_{1,-1}\ \mathbf{a}_{1,0}\ \mathbf{a}_{1,1}\ \ldots\ \mathbf{a}_{L_{\text{in}},L_{\text{in}}}] \tag{4.7}$$

and

$$\mathbf{S}_{\text{out}} = [\mathbf{b}_{1,-1}\ \mathbf{b}_{1,0}\ \mathbf{b}_{1,1}\ \ldots\ \mathbf{b}_{L_{\text{out}},L_{\text{out}}}] \tag{4.8}$$

The corresponding coordinates $\mathbf{x} = [\mathbf{x}_{\text{in}}^{\text{H}}\ \mathbf{x}_{\text{out}}^{\text{H}}]^{\text{H}}$

$$x_{\text{in},lm} = \alpha_{lm}, \tag{4.9}$$

$$x_{\text{out},lm} = \beta_{lm}. \tag{4.10}$$

Here the transpose is denoted as the Hermitian transpose H due to the coordinates being complex-valued.

Based on the expansion, Eq. (4.4), of the harmonic scalar potential V alone, one might think that the sensors would have to be located on a non-spherical array in order to produce non-singular SSS basis. This conclusion would arise from the fact that the internal and external part of the scalar expansion have exactly the same angular dependence. Publication II shows, however, that in the measurement of magnetic field derivable from V, the SSS basis is singular only if the normal vectors of the sensors are all either radial or tangential, even for sensors located on a perfectly spherical surface. Thus, the SSS basis separates the inside and outside contributions more clearly than an intuitive conclusion might suggest.

In practice, the modern multichannel MEG devices have a non-singular SSS basis since the sensors are located on a non-spherical surface and they are not strictly radial or tangential. Thus, the estimate $\hat{\mathbf{x}} = \mathbf{S}^{\dagger}\phi$ gives unique device-independent coordinates in the form

$$\hat{\mathbf{x}} = \begin{bmatrix} \hat{\mathbf{x}}_{\text{in}} \\ \hat{\mathbf{x}}_{\text{out}} \end{bmatrix} \tag{4.11}$$

Given a perfect calibration accuracy of the sensors and adequate spatial sampling, there is no mixing between the contributions of $\mathbf{J}_{\text{in}}$ and $\mathbf{J}_{\text{out}}$ because of the linear independence of the SSS basis vectors. Even with realistic calibration accuracy, this mixing is negligible if the expansion orders are sufficient, as will be shown in chapter 5.1.

All real measurements contain sensor noise. In MEG measurements, it is usually assumed that this noise is normally distributed and uncorrelated among the sensors, resulting in a diagonal covariance matrix. Application of SSS changes the sensor noise covariance $\mathbf{N}$, which can be taken into account if needed as shown in publication II. The brain noise, which dominates over the sensor noise especially below 60 Hz, is not affected by SSS since it is produced by currents in the internal volume defined by Fig. 2.1.

The condition number, defined as the ratio of the largest and smallest singular value of the SSS basis, is apparently very high due to the highly different scales of the different basis functions leading to a large range of norm values among the SSS basis vectors. The basis can be stabilized simply by normalizing $\mathbf{S}$, which usually gives a reasonable condition number, as discussed in publication IV. Further stabilization can be achieved by selecting only the basis functions that have strong enough coupling to the sensor array to exceed sensor noise (Nenonen *et al.*, 2007). When using normalized $\mathbf{S}$, the estimated coordinates $\hat{x}_{\mathrm{in},lm}$ can be converted to SI units by dividing them with norms $||\mathbf{a}_{lm}||$ of the non-normalized basis.

4.3 Coordinates for MEG: The magnetostatic multipole moments

As shown in publication II, the operation $\phi \rightarrow \hat{\mathbf{x}}$ transforms the multichannel measurement into the magnetostatic multipole moments that have a lead field representation

$$\alpha_{lm} = \ < \lambda^{\alpha}_{lm}, \mathbf{J}_{\mathrm{in}} > \ = \int_{v'} \lambda^{\alpha}_{lm}(\mathbf{r}') \cdot \mathbf{J}_{\mathrm{in}}(\mathbf{r}') dv', \tag{4.12}$$

where

$$\lambda^{\alpha}_{lm}(\mathbf{r}') = \frac{i}{2l+1}\sqrt{\frac{l}{l+1}} r'^{l} \mathbf{X}^{*}_{lm}(\theta', \varphi'). \tag{4.13}$$

The current distribution $\mathbf{J}_{\mathrm{in}}$ is enclosed by a sphere with radius R_{α}. Because of the orthonormality of the tangential VSH functions $\mathbf{X}_{lm}$ over a spherical surface, the lead fields λ^{α}_{lm} are orthogonal over the spherical volume enclosing the brain. Thus, Eq. (4.12) satisfies Eq. (3.10) and Eq. (3.11) thereby making the multipole moments a suitable choice for coordinates of MEG measurements. Alvarez (Alvarez, 1991) has proposed a method for extracting the multipole moments from a magnetic measurement conducted on a plane. He derives an expression equivalent with Eq. (4.13). In his expression the integrand contains $\mathbf{J} \cdot \mathbf{X}_{lm}$. However, with the current being real-valued, $\mathbf{J} \cdot \mathbf{X}_{lm} = (\mathbf{X}_{lm} \cdot \mathbf{J})^{*} = \mathbf{X}^{*}_{lm} \cdot \mathbf{J}$, which is compatible with Eq. (4.13).

The coordinate representation provided by the multipole moments has several advantages over the conventional approach of directly using the signals of the physical sensors in data analysis. In the multipole moments, all the information of the

magnetic field produced by the brain is packed into a compact representation corresponding to point-like sensors with orthogonal lead fields. Therefore, the number of multipole moments needed is smaller than the number of physical sensors. The forward modelling of the moments does not require any numerical integration as in calculation of the flux through the pick-up loop of the sensor. Throughout this thesis, it should be noted that the orthogonality of the multipole moments corresponds to spatial information and linear algebra, and should not be confused with statistical orthogonality or independence.

Furthermore, the multipole moments are device-independent and thus enable a straightforward calculation of virtual signals corresponding to different head positions and sensor arrays.

4.4 Spatiotemporal signal space separation (tSSS)

The spatial SSS performs in a satisfactory manner in typical MEG measurements. A good estimate $\hat{\mathbf{x}}$ is guaranteed when deviations ϕ_ϵ of the signal from the model in Eq. (4.6) are insignificant. Taking the deviations into account, the model is of the form

$$\phi = \mathbf{S}\mathbf{x} + \phi_\epsilon. \tag{4.14}$$

In addition to random sensor noise, such deviations can be produced by insufficient calibration accuracy of the sensor array causing erroneous elements in the basis matrix $\mathbf{S}$. Additional source of deviation is the presence of sources that produce detectable magnetic fields with spatial frequencies higher than those included in the basis $\mathbf{S}$ rendering the dimension of the basis matrix too small to correctly describe these fields. Such sources are typically artifact sources in the immediate vicinity of the sensors, e.g., stimulators or magnetized electrodes close to the head.

From Eq. (4.14) we get the estimate

$$\hat{\mathbf{x}} = \mathbf{S}^\dagger\phi = \mathbf{S}^\dagger\mathbf{S}\mathbf{x} + \mathbf{S}^\dagger\phi_\epsilon \equiv \mathbf{x} + \mathbf{x}_\epsilon, \tag{4.15}$$

where

$$\mathbf{x}_\epsilon = \begin{bmatrix} \mathbf{x}_{\mathrm{in},\epsilon} \\ \mathbf{x}_{\mathrm{out},\epsilon} \end{bmatrix} \tag{4.16}$$

Thus, the signal deviation ϕ_ϵ leaks into the internal and external signal contribution estimated by SSS. Temporally, $\mathbf{x}_{\mathrm{in},\epsilon}$ and $\mathbf{x}_{\mathrm{out},\epsilon}$ contain mutually equivalent temporal waveforms that are originally present in the signal deviation ϕ_ϵ. Assuming that the brain and external interference signals, both correctly modelled by the spatial SSS, are temporally uncorrelated, the only possible cause for temporal correlation between $\mathbf{x}_{\mathrm{in}}$ and $\mathbf{x}_{\mathrm{out}}$ is the above leakage phenomenon.

Removal of the contribution of ϕ_ϵ was developed and applied in publication III. First, the intersecting waveforms are identified by a singular value decomposition (SVD)

based subspace intersection estimation method. Then the intersecting waveforms are projected out in the time domain from the SSS-estimate of the internal signal. Consequently, the recognized signal deviations, usually caused by nearby artifacts, are suppressed below the noise level of the sensors. Recently, quite a similar method utilizing reference sensors, instead of SSS as the original separation method, has been proposed (de Cheveigné and Simon, 2007).

5 Applications of SSS and tSSS

5.1 Suppression of external interference

The estimated coordinates, i.e., the magnetostatic multipole moments of Eq. (4.11) allow one to suppress the contribution of external interference simply by omitting $\hat{\mathbf{x}}_{\text{out}}$ and considering $\hat{\mathbf{x}}_{\text{in}}$ only. These coordinates contain the measurable information generated by physiological currents in the brain. One can reconstruct the measurement as it would be in the absence of interference by

$$\hat{\phi}_{\text{in}} = Re(\mathbf{S}_{\text{in}}\hat{\mathbf{x}}_{\text{in}}), \tag{5.1}$$

where Re indicates the real part.

The sensitivity of $\hat{\mathbf{x}}$ to random noise and calibration errors depends on the condition number, defined as the ratio of the largest and smallest singular value, of the basis matrix $\mathbf{S}$. In SSS it is particularly important that the subspaces $\mathbf{S}_{\text{in}}$ and $\mathbf{S}_{\text{out}}$ differ clearly enough from each other in order to achieve a good estimate $\hat{\mathbf{x}}_{\text{in}}$. The spectrum of principal angles between the subspaces gives a measure of difference (Golub and Van Loan, 1996) between the internal and external bases. In publication IV the minimum, mean, and maximum principal angles were computed for three different sensor configurations with four reasonable (L_{in}, L_{out}) combinations. With the orders $L_{\text{in}} = 8$ and $L_{\text{out}} = 3$, the minimum, mean, and maximum principal angles for the 306-channel device are 5, 11, and 25 degrees, respectively. These values have turned out to be large enough in order to achieve good signal separation.

The condition number and principal angles of $\mathbf{S}$ affect the stability of the pseudoinverse $\mathbf{S}^{\dagger}$. A well-conditioned matrix tolerates reasonable measurement errors, either due to random noise or systematic inaccuracies in the information concerning the gains and geometry of the sensors. Publication IV demonstrates that in the basic implementation of SSS with the 306-channel device, the overall contribution of random noise is not significantly affected by the SSS reconstruction. On the other hand, calibration errors as small as 1 % result in shielding factor of about 15 only against external interference. Fortunately, calibration accuracy of about 0.1 % is achievable by a parameter search method minimizing the difference between measured signals and the SSS basis. With this accuracy, the shielding factor, achievable by the SSS method, clearly exceeds 100. Fig. 5.1 shows the computational shielding factors for different values of L_{out}. The asymptotic shielding factor decreases with increasing L_{out} as the condition number of $\mathbf{S}$ increases with its dimension.

Fig. 5.2 shows a practical example of the performance of SSS in interference suppression. Auditory evoked fields were recorded from a healthy subject in the presence of interference typical for a laboratory environment. The measurement was done in a

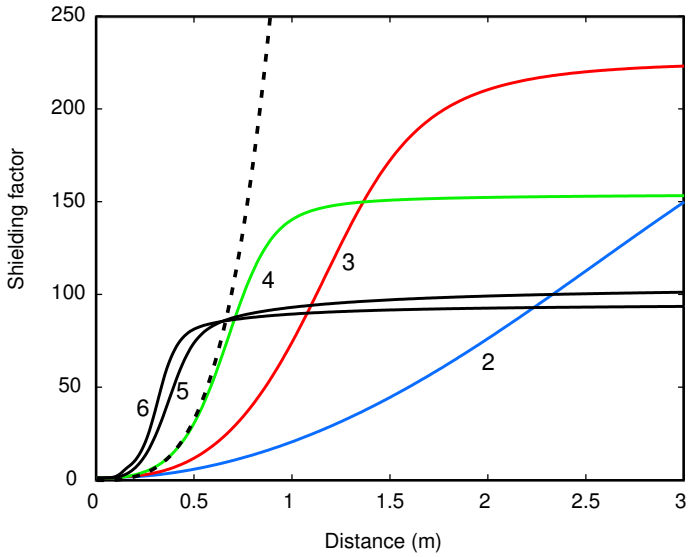

Figure 5.1: The shielding factor of SSS as a function of distance of the interference source from the center of the sensor array at different L_{out} values. The curves are based on a simulation corresponding to calibration accuracy of 0.1 % of the 306-channel MEG device. The dashed curve corresponds to $L_{\text{out}} = 4$ and perfect calibration accuracy.

magnetically shielded room whose door was left intentionally open for the duration of the recording. The averaged responses are dominated mostly by power-line interference especially on magnetometers but the gradiometers are also affected. SSS effectively suppresses the disturbances and reveals a clear brain response associated with a dipolar field pattern.

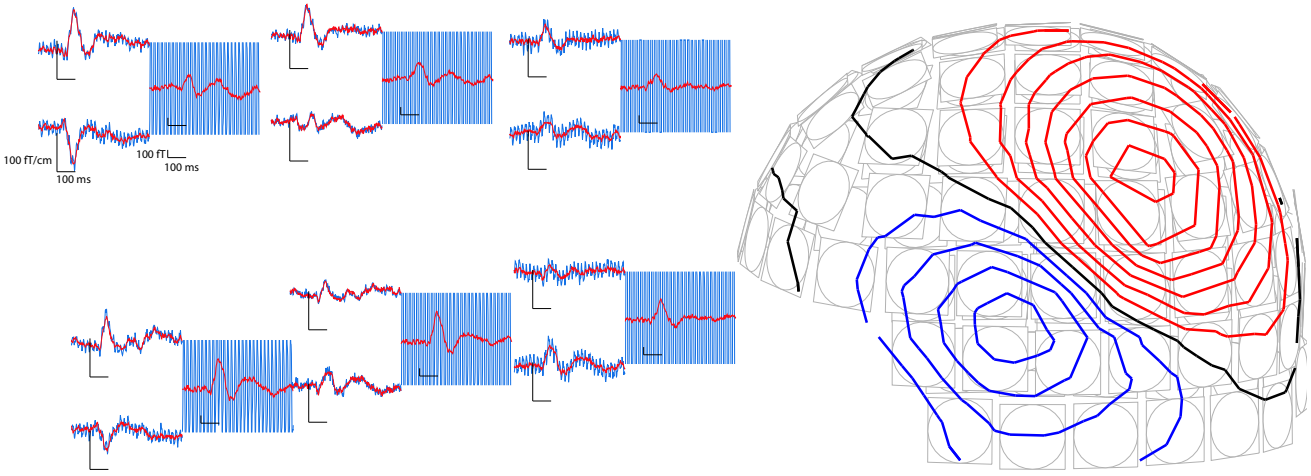

Figure 5.2: Left: the original (blue) and SSS-reconstructed (red) evoked auditory signals from a subset of channels. The channels are organized as triplets where the magnetometer is shown on the right and the orthogonal gradiometers are shown on the left. Right: the SSS-reconstructed field pattern at the time of the peak latency.

5.2 Standardization of MEG signals

The magnetostatic multipole vector $\mathbf{x}_{\text{in}}$ composed of the α_{lm} values offers dimensionality reduction, i.e., packing of data, and standardization of the MEG signals into a device-independent form. The former feature is achieved by the orthogonality of the lead fields λ_{lm} and the latter stems from the fact that the multipoles are attached to the coordinate system of the head.

The device-independence enables a simple method to transform the measured sensor-level signals into different head positions or sensor arrays. Instead of reconstructing the signals of the configuration used in the measurement, the basis matrix $\mathbf{S}_{\text{in}}$ is replaced by the basis $\mathbf{S}_{\text{in,v}}$ of the virtual configuration:

$$\phi_{\text{v}} = Re(\mathbf{S}_{\text{in,v}}\hat{\mathbf{x}}_{\text{in}}). \tag{5.2}$$

The transformation is limited by the information content of the actual measurement making it impossible to enhance the SNR of the measurement, e.g., by virtually

transforming the head position closer to the sensors. In such a transformation the increasing signal amplitude is associated with increasing sensor noise. This effect is quite insignificant in transformation between different head positions relatively close to each other as demonstrated by the example of head position standardization shown in Fig. 5.3 including four different head positions of an adult subject. Reduction of SNR in transformations over large distances can be controlled by the Wiener-like weighting method introduced in publication I.

5.3 Head movement compensation

The movement compensation can be considered time-dependent standardization of MEG signals. The changing head position is taken into account as a time-dependent SSS basis $\mathbf{S}(t)$. The compensated result in its simplest form is the estimate

$$\hat{\mathbf{x}}(t) = \mathbf{S}(t)^{\dagger}\phi(t). \tag{5.3}$$

Consequently, the dynamics related to the head movements is suppressed by SSS leaving only the time-dependence of brain activity in $\hat{\mathbf{x}}_{\mathrm{in}}(t)$. If desired, virtual signals corresponding to physical sensors and a standard head position can be reconstructed from $\hat{\mathbf{x}}_{\mathrm{in}}(t)$ by Eq. (5.2).

It was shown in publication II that if the head movement and brain signals can be assumed to be statistically independent, movement compensation of averaged signals simplifies to

$$\mathrm{E}[\hat{\mathbf{x}}] \;=\; \mathrm{E}[\mathbf{S}]^{\dagger}\mathrm{E}[\phi], \tag{5.4}$$

where E[·] indicates averaging over the consecutive trials. Thus, in this case it is sufficient to separately average the SSS basis and the signal vector.

The performance limits of SSS-based movement compensation were tested by the extreme case of randomly moving a small phantom head with movement ranging up to 15 cm. The dipole moment was 20 nAm and 500 responses were averaged. The head position monitoring was able to track the movement (Fig. 5.4) and compensation of the averaged dipole field using Eq. (5.4) followed by Eq. (5.2) demodulated the distortion caused by the movement. Consequently, the movement bias causing a dipole localization error of about 4 cm was reduced to give a location accuracy of approximately 4 mm. An example of movement compensation in a real auditory MEG measurement is demonstrated in publication IV.

5.4 Removal of nearby artifacts

Significant artifact sources in the proximity of the MEG sensors are quite common especially in clinical examinations. These disturbances arise from, e.g., VNS

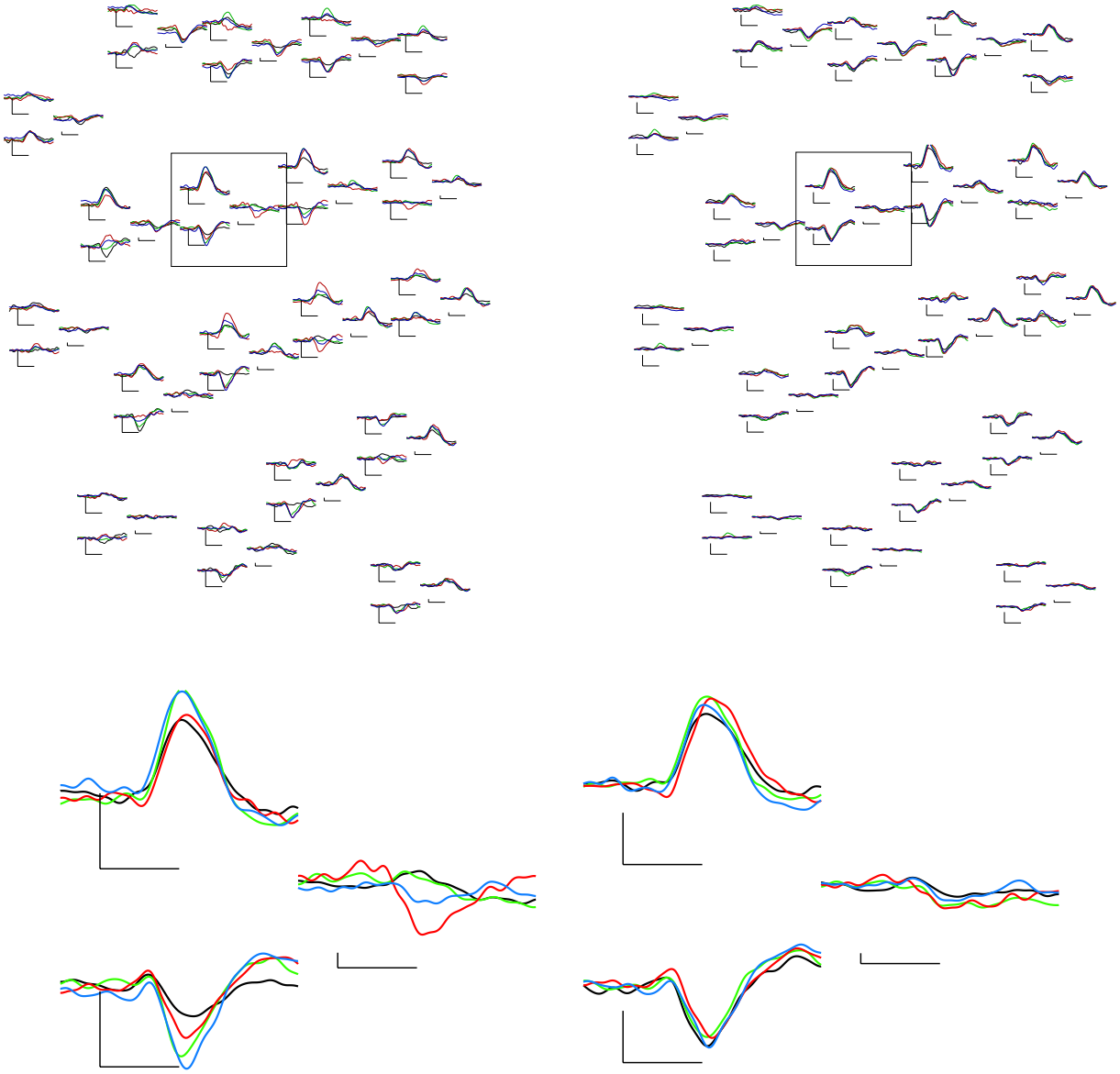

Figure 5.3: Auditory signals from a subset of channels corresponding to measurements with four different head positions. Left column: Original evoked responses. Right column: Evoked responses after standardizing the head positions with SSS. Blue, red, green, and black colours correspond to positions in the middle, left side, right sight, and slightly downward within the Elekta Neuromag® sensor array.

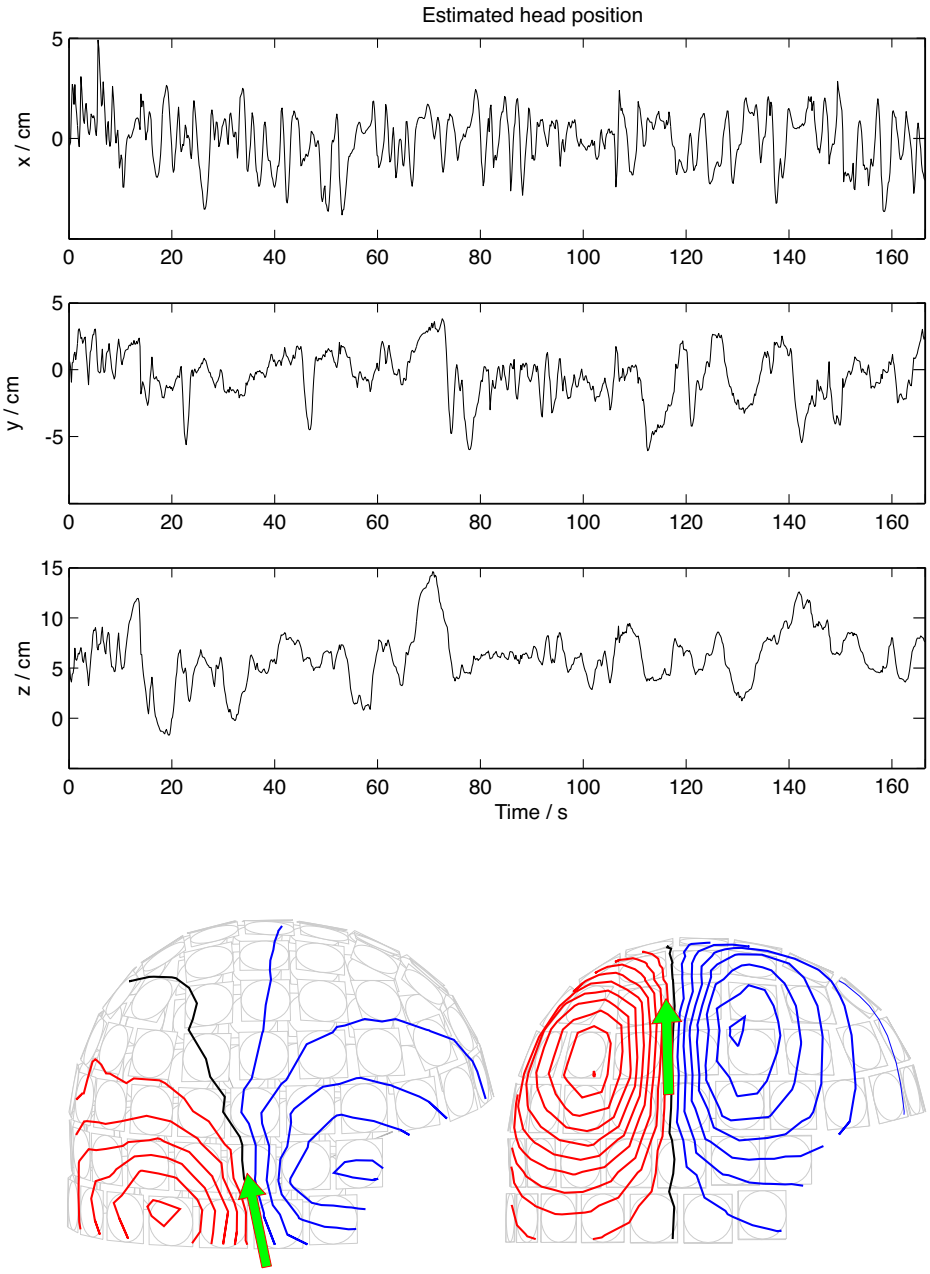

Figure 5.4: Top: Estimated time traces of phantom position when the phantom was intentionally moved. Lower left figure: The unprocessed averaged field pattern corresponding to repeated activation of an artificial current dipole in the phantom. Lower right figure: The movement-compensated field pattern from the same recording.

stimulators, magnetized dental work, EEG cables, or magnetic particles left on the skull from previous brain surgery. For the same reason, meaningful MEG scans on Parkinsonian patients treated with deep brain stimulators (DBS) have been traditionally considered impossible although some studies exist despite the large artifacts (Kringelbach *et al.*, 2007).

The tSSS method is especially efficient in removing artifacts caused by nearby sources even from sources located between the brain and the sensors. Publication V demonstrates that tSSS removes artifacts having varying spatial characteristics and enables one to examine single evoked responses without any additional signal processing. It is shown that the quality of the tSSS processed data is preserved as the spatial complexity of the artifact pattern is intentionally increased from normal environmental condition to additional external interference and finally to nearby artifacts generated by a magnetized object attached to subject's lip, see Fig. 5.5. The tSSS method has also been used in clinical measurements involving VNS and DBS stimulators (Taulu *et al.*, 2006; Mäkelä *et al.*, 2007).

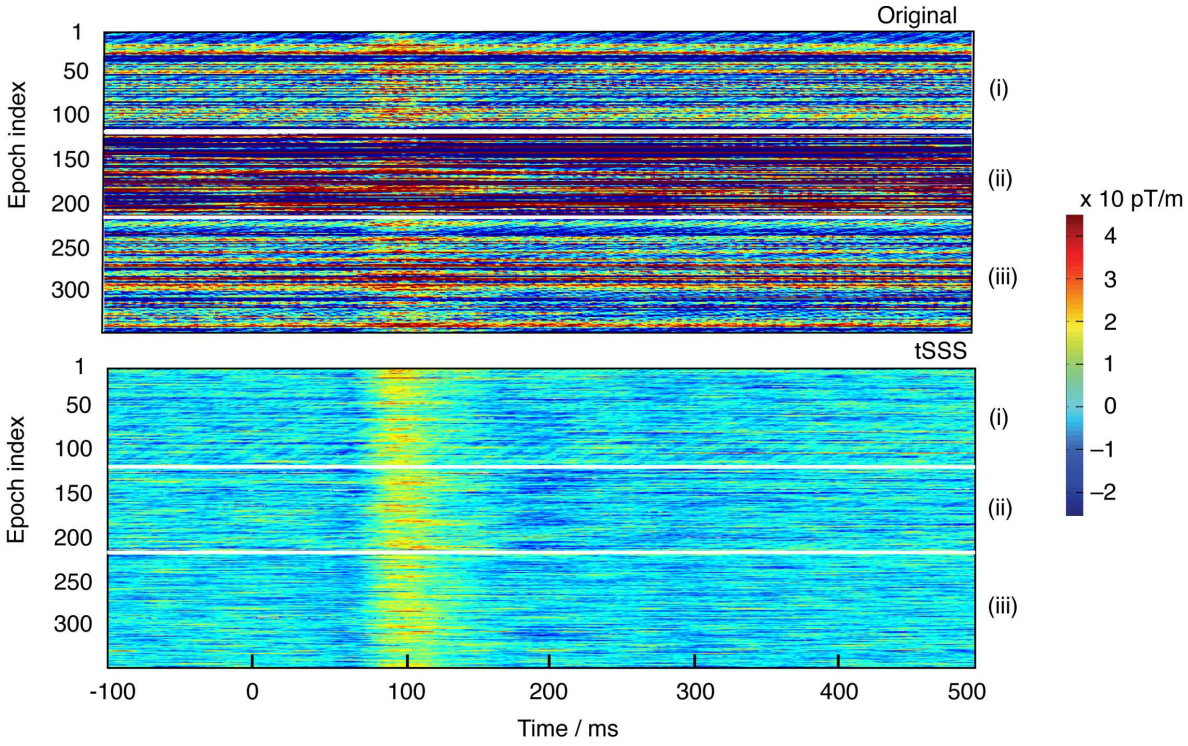

Figure 5.5: Consecutive single auditory responses from a single gradiometer channel containing original (upper figure) and tSSS reconstructed (bottom figure) data. In both figures, the epochs corresponding to control (i), additional external interference (ii), and nearby artifacts (iii) are separated by thin white lines.

The tSSS method is a very efficient method to remove interference from MEG measurements without *a priori* information about the artifacts. As in the case of SSS, source modelling of tSSS processed data can be done readily without having to take the processing into account in forward calculation algorithms. The sensor noise covariance $\mathbf{N}$, however, is modified by SSS and tSSS, but this can be taken into account, if needed, by using Eqs. 33 and 34 of publication II. Let us now denote this modified and known covariance as $\tilde{\mathbf{N}}$. The original total noise covariance is

$$\mathbf{N}_{\mathrm{tot}} = \mathbf{N}_{\mathrm{brain}} + \mathbf{N}, \tag{5.5}$$

where $\mathbf{N}_{\mathrm{brain}}$ is the covariance due to brain noise that dominates over $\mathbf{N}$ at frequencies below 60 Hz. After SSS, the covariance is

$$\tilde{\mathbf{N}}_{\mathrm{tot}} = \mathbf{N}_{\mathrm{brain}} + \tilde{\mathbf{N}}. \tag{5.6}$$

The expression for $\tilde{\mathbf{N}}$ is given in publication II and the actual noise properties of common MEG systems are described in publication IV. Because of the dominating role of $\mathbf{N}_{\mathrm{brain}}$, the change from $\mathbf{N}_{\mathrm{tot}}$ to $\tilde{\mathbf{N}}_{\mathrm{tot}}$ is not significant in practice.

The drawback of tSSS as compared to SSS is that the former method is computationally more extensive and involves temporal processing that, in principle, may alter the temporal pattern of the brain signals. This problem can be avoided by selecting the time window of tSSS properly as discussed in publication V.

5.5 Source modelling with multipole moments

The idea of using the multipole expansion as a model for extended sources has been proposed and studied previously (see, e.g., Karp *et al.*, 1980; Katila, 1983; Jerbi *et al.*, 2002). In contrast to those methods utilizing a low-order multipole expansion as a source model for a limited portion of the cortex or the heart, publications I and II show the derivation and demonstration of source modelling based on multipole moments α_{lm} corresponding to the whole brain. The idea is based on the ability of the SSS method to transform the whole multichannel measurement into a set of magnetostatic multipole moments having orthogonal lead fields corresponding to the total current, see Eq. (4.11) - Eq. (4.13).

The multipole moments α_{lm} represent the MEG data in the form of standardized and device-independent virtual channels. Existing source modelling methods can be used on the α_{lm} values by replacing the forward model of the physical sensors with that corresponding to Eq. (4.12). The multipole moments offer a simple model as they can be considered point-like virtual sensors that do not require surface integration unlike the physical sensors whose pick-up loops need to be modelled. In the case of SSS, this modelling takes place in the computation of the SSS basis matrix that needs to be updated once for each head position.

The analytic and orthogonal lead fields of the multipole moments correspond directly to the total current $\mathbf{J}_{\rm in}(\mathbf{r}')$. Thus, the multipole moments couple to $\mathbf{J}_{\rm in}(\mathbf{r}')$ with a mathematical expression allowing one to derive a general estimate for $\mathbf{J}_{\rm in}(\mathbf{r}')$ in a least-squares sense to explain the measured data, as shown in publications I and II. This estimate is of the form

$$\mathbf{J}_{\rm in}(\mathbf{r}') = \sum_{l=1}^{\infty} \sum_{m=-l}^{l} \alpha_{lm} \eta_l \left(\frac{r'}{R_\alpha} \right)^l \mathbf{X}^*_{lm}(\theta', \varphi'), \tag{5.7}$$

where R_α is the radius of the sphere enclosing the current, and

$$\eta_l = -i(2l+1)(2l+3)\sqrt{\frac{l+1}{l}} \frac{1}{R_\alpha^{l+3}}. \tag{5.8}$$

This estimate does not make any reference to the conductor geometry whose effect is inherently included in the measured multipole moments α_{lm}. The physiologically generated primary current $\mathbf{J}^{\rm p}$ does not depend on the conductor volume unlike the associated passive volume current $\mathbf{J}^{\rm v}$. Both of these contributions show up in the α_{lm} values and need not be modelled explicitly. Fig. 5.6 shows an example of the total current estimate in a real evoked response corresponding to auditory stimulation. Here the norm $||\mathbf{J}_{\rm in}||^6$ is used for visualization purposes. One should note, however, that this estimate is more sensitive to noise than the norm $||\mathbf{J}_{\rm in}||^2$.

5.6 Other applications

The SSS-based transformation of the multichannel data into an orthogonal coordinate representation is useful also in many applications not described above. One of them is the active compensation system utilizing coils inside the MSR to produce compensating signals for the external interference based on feedback received from actual MEG sensors. While suppressing the interference, the coils apparently distort the brain signal as well, which can be reconstructed by SSS that removes the contribution of the coils located outside the sensor array. The active compensation method enables MEG measurements with lighter MSRs that fit into standard office space.

Direct current (DC) or near-DC signals are of interest, e.g., in migraine and head trauma studies; for a review, see (Cohen, 2004). The SQUID sensors, however, are insensitive to static fields and signals at very low frequencies are prone to strong interference. These problems can be alleviated by modulating the low-frequency signals to higher frequencies by moving the head with respect to the sensors. One solution is to move the subject in a controlled manner using a moving bed (Mackert *et al.*, 1999). SSS-based movement compensation allows measurement of DC signals that are modulated by the unrestricted voluntary movement of the head (Taulu *et*

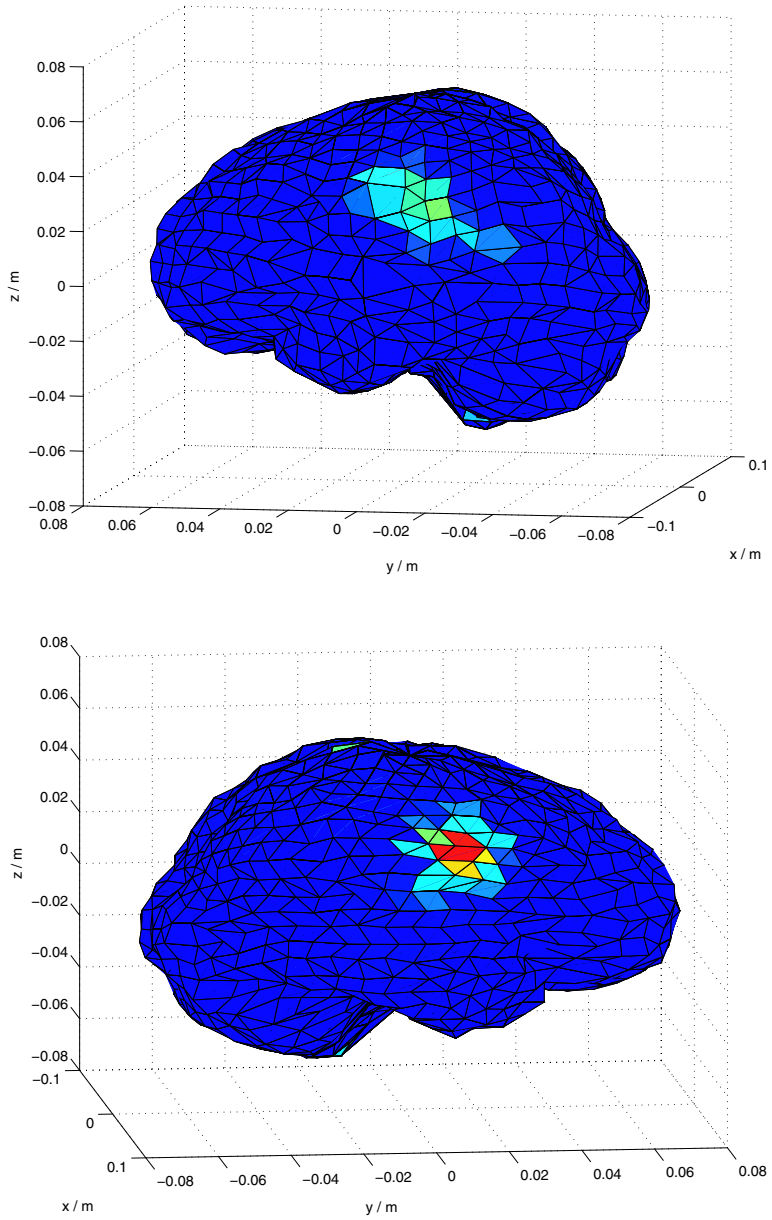

Figure 5.6: The normalized total current $||\mathbf{J}_{\text{in}}||^6$ corresponding to an auditory evoked field. The current $||\mathbf{J}_{\text{in}}||$ was projected to the mesh surface.

al., 2004). Thus, the need for special instrumentation to create the movement is avoided.

In publication IV, it was demonstrated that a calibration accuracy on the order of 0.1 % is achieved based on SSS. Briefly, calibration of a multichannel device can be represented as finding a set of calibration parameters that are optimal in the sense that they minimize some distance function $d(\Phi, \mathbf{M})$ between the measurement Φ and some model signal $\mathbf{M}$ that the measurement is assumed to obey. Typically, the model signal is produced by a specially constructed calibration source or phantom (see, e.g., Hall Barbosa *et al.*, 1999; Ornelas *et al.*, 2003). The calibration parameters are then adjusted to minimize the difference between the measured signals and the forward model of the calibration source in a least-squares sense. The accuracy of calibration based on a restricted calibration signal is limited by the accuracy of the forward model and, especially, the geometrical precision of the calibration source regarding its manufacturing and positioning with respect to the MEG device. In practice, accuracy better than a few percent is difficult to achieve with this approach. In the SSS-based calibration, the model $\mathbf{M}$ is the SSS basis. Thus, instead of calibrating against a certain calibration source, one calibrates directly against Maxwell's equations, provided that the basic assumptions of SSS are valid, i.e., there are no sources of magnetic field in the sensor volume and the measured fields correspond to relatively low spatial frequencies. The calibration can be implemented, e.g., by measuring strong environmental signals containing magnetic fields in all three spatial directions and at different spatial frequencies. Then, the parameters describing the gains and the geometry of the device are fitted by simulated annealing, simplex, or an equivalent algorithm to minimize the subspace angle between Φ and $\mathbf{S}$. When the angle is at minimum, the SSS model is consistent with the measured signals produced by magnetic fields known to obey Maxwell's equations.

6 Conclusions

This thesis describes solutions to some of the most prevalent signal processing problems of MEG. The basic idea is the transformation of the multichannel data into a set of spatially uncorrelated components that correspond to brain signals only and are device-independent. The method is successful in MEG utilizing modern multichannel devices but can also be used in other magnetic multichannel measurement technologies, such as MCG or geomagnetism. Publication I describes the general idea of representing a multichannel signal as a set of coordinates in a suitable signal subspace, analogous to representing the three dimensional location of an object by the Cartesian coordinates. Compatible with this framework, publication II describes the mathematics of the SSS method that transforms the multichannel signals into device-independent multipole moments with separate sets of moments for the brain signals and external interference. Publication III introduces the temporal extension (tSSS) to the spatial SSS, which is needed for the artifact removal in cases with very strong interference or artifact sources located very close to the sensors. Publications IV and V demonstrate the applications of SSS and tSSS with simulated and real data.

The output of the SSS transformation contains the measured information in a form attached to the coordinate system of the head and with the contributions of the external interference sources suppressed. Thus, SSS and tSSS reconstructions simultaneously perform artifact suppression, position standardization, and movement compensation. Furthermore, the standardized result is more tractable for source analysis than the original signal values of the physical sensors. The method is based on the harmonic analysis of the magnetic flux density based on Maxwell's equations in free space. It has been shown to be a robust tool in MEG largely due to the fact that it is based on fundamental and well-known laws of physics with few assumptions, a condition only possible for modern multichannel devices providing extensive oversampling of the biomagnetic field. The methods presented in this thesis are already in use by several investigators. After the first introduction of the idea of SSS (Taulu *et al.*, 2003), the earliest studies in basic brain research utilizing this method have been in infant MEG (Cheour *et al.*, 2004; Pihko *et al.*, 2004). Investigations concerning head position standardization and movement compensation have also been carried out (see, e.g., Lioumis *et al.*, 2007; Medvedovsky *et al.*, 2007; Wehner *et al.*, 2008). Clinical studies have so far concerned epilepsy and Parkinson's disease (Taulu *et al.*, 2006; Mäkelä *et al.*, 2007). tSSS is expected to be especially important in clinical examinations as it opens the possibility to study certain patient groups traditionally excluded from MEG. Such cases are, e.g., patients with magnetic contamination in the skull and patients treated with stimulators like VNS or DBS.

The method has also commercial potential. Elekta Neuromag Oy's MaxFilter^{TM}

software product is based on SSS and tSSS and it is already in routine use in MEG signal processing. In addition, this software is an essential part of Elekta Neuromag Oy's single-shell MSR, MaxShield^{TM}, which has already been installed at eight sites in Europe and the United States. These products involve six patent applications (FI115324, FI115737, FI115736, FI20040233, FI20050445, US11/654029) related to SSS or tSSS, three of which have been granted so far.

The SSS method is not restricted to MEG. It can be extended to any other measurement technique where the signals can be represented as a linear combination of harmonic basis functions. Such measurements could be, e.g., different biomagnetic applications, and geomagnetic measurements using sensors on the terrestrial stations and in the satellites.

The main limitation of SSS is its sensitivity to the calibration accuracy of the measurement device and requirement for a relatively large number of sensors (Nurminen *et al.*, 2008), although it has been shown to be feasible for a device with only 76 channels (Okada *et al.*, 2006). To be suitable for SSS, special care has to be taken in the precision of the manufacturing and calibration processes of the device. tSSS is less sensitive to the calibration errors than SSS but it is also more time-consuming. Currently, SSS and tSSS are offline processes but means enabling their on-line usage are being developed.

The SSS and tSSS methods are still under development. Especially the noise optimization of the SSS method, optimization of the sensor array, and the criteria for the optimal choice of tSSS parameters will be studied. The coordinate representation supported by SSS provides interesting topics for future research. Among these, the usage of the multipole moments in conjunction with Shannon's information theory has been briefly studied (Nenonen *et al.*, 2007). Novel and efficient source modelling algorithms based on the multipole-related coordinate representation are also likely to emerge, for example by further developing the basic current distribution estimate of publication I. The simple representation of the measured data by the coordinates also provides efficient tools to model the information captured by the physical sensors. This can be used in design of improved sensor arrays that, in turn, provide increased stability for the SSS basis with subsequently improved suppression of external interference and optimized overall SNR of the SSS reconstruction. This may prove useful especially in studies of single-trial evoked responses.

7 References

Abramowitz M and Stegun A, 1964. Handbook of Mathematical Functions with Formulas, Graphs, and Mathematical Tables. Dover, New York.

Ahonen A I, Hämäläinen M S, Kajola M J, Knuutila E T, Laine P P, Lounasmaa O V, Simola J T, Tesche C D, and Vilkman V A, 1992. A 122-channel magnetometer covering the whole head. In: Dittmar A and Froment J C, editors, Proceedings of the Satellite Symposium on Neuroscience and Technology, 14th Annual Conference of the IEEE Engineering in Medicine and Biology Society, pages 16-20, IEEE Engineering and Medicine and Biology Society, Lyon.

Ahonen A, Hämäläinen M, Ilmoniemi R, Kajola M, Knuutila J, Simola J, and Vilkman V, 1993. Sampling theory for neuromagnetic detector arrays. IEEE Trans Biomed Eng 40, 859-869.

Alvarez R E, 1991. Filter functions for computing multipole moments from the magnetic field normal to a plane. IEEE Trans Med Imag 10, 375-381.

Arfken G, 1985. Mathematical Methods for Physicists. Academic Press, San Diego.

Barth D, Sutherling W, Engel J, and Beatty J, 1982. Neuromagnetic localization of epileptiform spike activity in the human brain. Science 218, 891-894.

Bork J, Hahlbohm H D, Klein R, and Schnabel A, 2001. The 8-layered magnetically shielded room of the PTB: Design and construction. In: Nenonen J, Katila T, and Ilmoniemi R J, editors, Proceedings of the 12th International Conference on Biomagnetism, pages 970-973. Helsinki University of Technology, Espoo, Finland.

Brenner D, Williamson S J, and Kaufman L, 1975. Visually evoked magnetic fields of the human brain. Science 190, 480-482.

Brenner D, Lipton J, Kaufman L, and Williamson S J, 1978. Somatically evoked magnetic fields of the human brain. Science 199, 81-83.

Burghoff M, Nenonen J, Trahms L, and Katila T, 2000. Conversion of magnetocardiographic recordings between two different multichannel SQUID devices, IEEE Trans Biomed Eng 47, 869-875.

Cheour M, Imada T, Taulu S, Ahonen A, Salonen J, and Kuhl P, 2004. Magnetoencephalography is feasible for infant assessment of auditory discrimination. Exp Neurol 190, S44-S51.

Cohen D, 1968. Magnetoencephalography: Evidence of magnetic fields produced by

alpha-rhythm currents. Science 161, 784-786.

Cohen D, 1970. Large-volume conventional magnetic shields. Rev Phys Appl 5, 53-58.

Cohen D, 1972. Magnetoencephalography: Detection of the brain's electrical activity with a superconducting magnetometer. Science 175, 664-666.

Cohen D, 2004. DC magnetic fields from the human body generally: a historical overview. Neurol Clin Neurophysiol 93.

de Cheveigné A and Simon J, 2007. Denoising based on time-shifted PCA. J Neurosci Meth 165, 297-305.

Dale A and Sereno M, 1993. Improved localization of cortical activity by combining EEG and MEG with MRI cortical surface reconstruction: A linear approach. J Cogn Neurosci 5, 162-176.

Fujinawa Y and Takahashi K, 1998. Electromagnetic radiations associated with major earthquakes. Phys Earth Plan Int 105, 249-259.

Gallen C, Sobel D, Waltz T, Aung M, Copeland B, Schwartz B, Hirschkoff E, and Bloom F, 1993. Noninvasive presurgical neuromagnetic mapping of somatosensory cortex. Neurosurgery 33, 260-268.

Gauss C and Weber W, 1839. Allgemeine Theorie des Erdmagnetismus, in "Resultate aus den Beobachtungen des magnetischen Vereins im Jahre 1838", publ C. F. Gauss and W. Weber Leipzig 1839 (English translation by Mrs. Sabine, revised by Sir John Herschel, "Scientific Memoirs," (R. Taylor ed.), 2, 184-251, London, 1841).

Garland, 1979. The contributions of Carl Friedrich Gauss to geomagnetism. Historia Mathematica 6, 5-29.

Geller R J, 1997. Earthquake prediction: a critical review. Geophys J Int 131, 425-450.

George M S, Sackeim H A, Rush A J, Marangell L B, Nahas Z, Husain M M, Lisanby S, Burt T, Goldman J, and Ballenger J C, 2000. Vagus nerve stimulation: a new tool for brain research and therapy. Biol Psychiatry 47, 287-295.

Golub G H and Van Loan C F, 1996. Matrix computations. John Hopkins, Baltimore.

Hall Barbosa C, Andrade Lima E, Bruno A C, Ewing A P, and Wikswo, J.P., Jr., 1999. Flux/voltage calibration of axial SQUID gradiometers using an optimization

procedure. IEEE Trans App Supercond 9, 3523-3526.

Hämäläinen M, Hari R, Ilmoniemi R J, Knuutila J, and Lounasmaa O V, 1993. Magnetoencephalography – theory, instrumentation, and applications to noninvasive studies of the working human brain. Rev Mod Phys 65, 413-498.

Hämäläinen M and Ilmoniemi R J, 1994. Interpreting magnetic fields of the brain: Minimum norm estimates. Med Biol Eng Comput 32, 35-42.

Hansen P C, 2006. Rank deficient and discrete ill-posed problems: numerical aspects of linear inversion. SIAM, Philadelphia.

Hari R, Aittoniemi K, Järvinen M L, Katila T, and Varpula T, 1980. Auditory evoked transient and sustained magnetic fields of the human brain: Localization of neural generators. Exp Brain Res 40, 237-240.

Hari R, Ahonen A, Forss N, Granström M-L, Hämäläinen M, Kajola M, Knuutila J, Lounasmaa O V, Mäkelä J P, Paetau R, Salmelin R, and Simola J, 1993. Parietal epileptic mirror focus detected with a whole-head neuromagnetometer. Neuroreport 5, 45-48.

Helmholtz H von, 1853. Ueber einige Gesetze der Vertheilung elektrischer Ströme in körperlichen Leitern, mit Anwendung auf die thierisch-elektrischen Versuche. Ann Phys Chem 89, 211-233, 353-377.

Hill E L, 1954. The theory of vector spherical harmonics. Am J Phys 22, 211-214.

Hochwald B and Nehorai A, 1997. Magnetoencephalography with diversely oriented and multicomponent sensors. IEEE Trans Biomed Eng 44, 40-50.

Ilmoniemi R, 1981. 7-channel SQUID magnetometer for brain research. MS.c. thesis, Helsinki University of Technology.

Ilmoniemi R, Hari R, and Reinikainen K, 1984. A four-channel SQUID magnetometer for brain research. Electroenceph Clin Neurophysiol 58, 467-473.

Ilmoniemi R J, 1985. Neuromagnetism: Theory, techniques, and measurements. Ph.D. thesis, Helsinki University of Technology.

Ilmoniemi R J, Hämäläinen M, and Knuutila J, 1985. The forward and inverse problems in the spherical model. In: Weinberg H, Stroink G, and Katila T, editors, Biomagnetism: Applications & Theory, pages 278-282. Pergamon, New York.

Ilmoniemi R J and Williamson S J, 1987. Analysis of the magnetic alpha rhythm in signal space. Soc Neurosci Abstr 13, 46.

Ilmoniemi R J, Williamson S J, and Hostetler W E, 1987. New method for the study of spontaneous brain activity. In: Atsumi K, Kotani M, Ueno S, Katila T, and Williamson S J, editors, Biomagnetism 87, pages 182-185. Tokyo Denki University Press, Tokyo.

Imada T, Zhang Y, Cheour M, Taulu S, Ahonen A, and Kuhl P, 2006. Infant speech perception activates Broca's area: a developmental magnetoencephalography study. Neuroreport 17, 957-962.

Ioannides A, Bolton J, Clarke C, 1990. Continuous probabilistic solutions to the biomagnetic inverse problem. Inverse Problems 6, 523-542.

Jackson J D, 1999. Classical Electrodynamics. John Wiley & Sons, Inc.

Jerbi K, Mosher J C, Baillet S, and Leahy R M, 2002. On MEG forward modelling using multipolar expansions. Phys Med Biol 47, 523-555.

Josephson B D, 1962. Possible new effects in superconductive tunnelling. Phys Lett 1, 251-253.

Kajola M, Ahlfors S, Ehnholm G J, Hällström J, Hämäläinen M S, Ilmoniemi R J, Kiviranta M, Knuutila J, Lounasmaa O V, Tesche C D, and Vilkman V, 1989. A 24-channel magnetometer for brain research. In: Williamson S J, Hoke M, Stroink G, and Kotani M, editors, Advances in Biomagnetism, pages 673-676, New York. Plenum.

Karp P J, Katila T E, Saarinen M, Siltanen P, and Varpula T T, 1980. The normal human magnetocardiogram. II. A multipole analysis. Circ Res 47, 117-130.

Katila T E, 1983. On the current multipole presentation of the primary current distributions. Il Nuovo Cimento 2D, 660-664.

Kelhä V O, Pukki J M, Peltonen R S, Penttinen A J, Ilmoniemi R J, and Heino J J, 1982. Design, construction, and performance of a large-volume magnetic shield. IEEE Trans Magn MAG-18, 260-270.

Knuutila J, Ahlfors S, Ahonen A, Hällström J, Kajola M, Lounasmaa O V, Vilkman V, and Tesche C, 1987. Large-area low-noise seven-channel dc SQUID magnetometer for brain research. Rev Sci Instrum 58, 2145-2156.

Kringelbach M L, Jenkinson N, Owen S L, and Aziz T Z, 2007. Translational principles of deep brain stimulation. Nat Rev Neurosci 8, 623-635.

Lesur V, 2006. Introducing localized constraints in global geomagnetic field modelling. Earth Planets and Space 58, 477-483.

Lioumis P, Taulu S, Kičić D, Nurminen J, Kähkönen S, Nenonen J, and Montonen J, 2007. Standardization of MEG sensors by the signal space separation method. Int Congr Ser 1300, 237-240.

Lounasmaa O V, 1974. Experimental principles and methods below 1 K, Academic, London.

Mackert B M, Wuebbeler G, Burghoff M, Marx P, Trahms L, Curio G, 1999. Non-invasive long-term recordings of cortical 'direct current' (DC-) activity in humans using magnetoencephalography. Neurosci Lett 273, 159-162.

Mäkelä J, Forss N, Jääskeläinen J, Kirveskari E, Korvenoja A, and Paetau R, 2006. Magnetoencephalography in neurosurgery. Neurosurgery 59, 493-510.

Mäkelä J, Taulu S, Pohjola J, Ahonen A, and Pekkonen E, 2007. Effects of subthalamic nucleus stimulation on spontaneous sensorimotor MEG activity in a Parkinsonian patient. Int Congr Ser 1300, 345-348.

Malmivuo J, 1976. On the detection of the magnetic heart vector - an application of the reciprocity theorem. Acta Polytechnica Scandinavica, Electrical Engineering Series No. 39. The Finnish Academy of Technical Sciences, Helsinki.

Matsuura K and Okabe U, 1995. Selective minimum-norm solution of the biomagnetic inverse problem. IEEE Trans Biomed Eng 42, 608-615.

Medvedovsky M, Taulu S, Bikmullina R, and Paetau R, 2007. Artifact and head movement compensation in MEG, Neurology Neurophysiology and Neuroscience 2007:4 (October 29, 2007).

Mosher J C, Lewis P S, and Leahy R M, 1992. Multiple dipole modeling and localization from spatio-temporal MEG data. IEEE Trans Biomed Eng 39, 541-557.

Naddeo A, Della Penna S, Nappi C, Vardaci E, and Pizzella V, 2002. Sampling and reconstruction schemes for biomagnetic sensor arrays. Phys Med Biol 47, N239-N248.

Nenonen J and Katila T, 1991. Noninvasive functional localization by biomagnetic methods, part I. J Clin Eng 16, 423-434.

Nenonen J, Purcell C J, Horacek B M, Stroink G, and Katila T, 1991. Magnetocardiographic functional localization using a current dipole in a realistic torso. IEEE Trans Biomed Eng 38, 658-664.

Nenonen J, Kajola M, Simola J, and Ahonen A, 2004. Total information of multi-

channel MEG sensor arrays. In: Halgren E, Ahlfors S, Hämäläinen M, Cohen D, editors, Proceedings of the 14th International Conference on Biomagnetism, pages 630-631. Biomag Ltd., Boston.

Nenonen J, Taulu S, Kajola M, and Ahonen A, 2007. Total information extracted from MEG measurements. Int Congr Ser 1300, 245-248.

Nishitani N and Hari R, 2002. Viewing lip forms: Cortical dynamics. Neuron 36, 1211-1220.

Nolte G, Fieseler T, and Curio G, 2001. Perturbative analytical solutions of the magnetic forward problem for realistic volume conductors. J Appl Phys 89, 2360-2369.

Numminen J, Ahlfors S, Ilmoniemi R, Montonen J, and Nenonen J, 1995. Transformation of multichannel magnetocardiographic signals to standard grid form. IEEE Trans Biomed Eng 42, 72-78.

Nurminen J, Taulu S, and Okada Y, 2008. Effects of sensor calibration, balancing and parametrization on the signal space separation method. Phys Med Biol 53, 1975-1987.

Nyquist H, 1928. Certain topics in telegraph transmission theory", Trans. AIEE, 47, 617-644.

Okada Y, Pratt K, Atwood C, Mascarenas A, Reineman R, Nurminen J, and Paulson D, 2006. BabySQUID: A mobile, high-resolution multichannel magnetoencephalography system for neonatal brain assessment. Rev Sci Instr 77, 024301 1-9.

Ornelas P H, Bruno A C, Hall Barbosa C, Andrade Lima E, and Costa Ribeiro P, 2003. A survey of calibration procedures for SQUID gradiometers. Supercond Sci Technol 16, 427-431.

Paetau R, Kajola M, and Hari R, 1990. Magnetoencephalography in the study of epilepsy. Neurophysiol Clin 20, 169-187.

Paetau R, 2008. Private communication.

Pascual-Marqui R D, Michel C M, and Lehmann D, 1994. Low-resolution electromagnetic tomography: A new method for localizing electrical activity in the brain. Int J Psychophysiol 18, 49-65.

Pihko E, Lauronen L, Wikström H, Taulu S, Nurminen J, Kivitie-Kallio S, and Okada Y, 2004. Somatosensory evoked potentials and magnetic fields elicited by

tactile stimulation of the hand during active and quiet sleep in newborns. Clin Neurophysiol 115, 448-455.

Plonsey R and Heppner D B, 1967. Considerations of quasistationarity in electrophysiological systems. Bull Math Biophys 29, 657-664.

Rabinovitch A, Frid V, and Bahat D, 2007. Surface oscillations – A possible source of fracture induced electromagnetic radiation. Tectonophysics 431, 15-21.

Rodriguez-Oroz M C, Obeso J A, Lang A E, Houeto J -L, Pollak P, Rehncrona S, Kulisevsky J, Albanese A, Volkmann J, Hariz M I, Quinn N P, Speelman J D, Guridi J, Zamarbide I, Gironell A, Molet J, Pascual-Sedano B, Pidoux B, Bonnet A M, Agid Y, Xie J, Benabid A L, Lozano A M, Saint-Cyr J, Romito L, Contarino M F, Scerrati M, Fraix V, and Van Blercom N, 2005. Bilateral deep brain stimulation in Parkinson's disease: a multicentre study with 4 years follow-up. Brain 128, 2240-2249.

Romani G L, Leoni R, and Salustri C, 1985. Multichannel instrumentation for biomagnetism. In: Hahlbohm H D and Lübbig H, editors, SQUID '85: Superonducting quantum interference devices and their applications, pages 919-932. Walter de Gruyter, Berlin.

Ryhänen T, Seppä H, Ilmoniemi R, and Knuutila J, 1989. SQUID magnetometers for low-frequency applications. J Low Temp Phys 76, 287-386.

Sabaka T J, Olsen N, and Purucker M E, 2004. Extending comprehensive models of the Earth's magnetic field with Ørsted and CHAMP data. Geophys J Int 159, 521-547.

Sarvas J, 1987. Basic mathematical and electromagnetic concepts of the biomagnetic inverse problem. Phys Med Biol 32, 11-22.

Scherg M, 1990. Fundamentals of dipole source potential analysis. In: Grandori F, Hoke M, and Romani G L, editors, Auditory Evoked Magnetic Fields and Electric Potentials, pages 40-69. Karger, Basel. Vol. 6 of Advances in Audiology.

Shannon C E, 1948. A mathematical theory of communication. The Bell System Technical Journal 27, 379-423, 623-656.

Shannon C E, 1949. Communication in the presence of noise. Proc IRE 37, 10-21.

Shibasaki H, Ikeda A, and Nagamine T, 2007. Use of magnetoencephalography in the presurgical evaluation of epilepsy patients. Clin Neurophys 118, 1438-1448.

Tank S B, 2000. Rotation of the geomagnetic field about an optimum pole. Geo-

phys J Int 140, 461-464.

Taulu S, Kajola M, and Simola J, 2003. The signal space separation method. Abstract book of the NFSI2003 conference, page A79, Chieti, Italy.

Taulu S, Simola J, and Kajola M, 2004. MEG recordings of DC fields using the signal space separation method (SSS). Neurol Clin Neurophysiol 35.

Taulu S, Paetau R, and Lauronen L, 2006. Artifact rejection of MEG data in pediatric epilepsy. Abstract book of the NCCN2006 conference, page 80, Helsinki, Finland.

Teyler T J, Cuffin B N, and Cohen D, 1975. The visual evoked magnetoencephalogram. Life Sci 17, 683-691.

Tiihonen J, Kajola M, and Hari R, 1989. Magnetic mu rhythm in man. Neurosci 32, 793-800.

Tripp J H, 1983. Physical concepts and mathematical models. In: Williamson S J, Romani G L, Kaufman L, and Modena I, editors, Biomagnetism: an interdiscplinary approach, pages 101-139. Plenum, New York.

Tuomisto T, Hari R, Katila T, Poutanen T, and Varpula T, 1983. Studies of auditory evoked magnetic and electric responses: Modality specificity and modelling. Il Nuovo Cimento 2D, 471-483.

Uusitalo M A and Ilmoniemi R J, 1997. Signal-space projection method for separating MEG or EEG into components. Med Biol Eng Comput 35, 135-140.

Uutela K, Hämäläinen M, and Somersalo E, 1999. Visualization of magnetoencephalographic data using minimum current estimates. NeuroImage 10, 173-180.

Uutela K, Taulu S, and Hämäläinen M, 2001. Detecting and correcting for head movements in neuromagnetic measurements. NeuroImage 14, 1424-1431.

Vrba J and Robinson S, 2001. Signal processing in magnetoencephalography. Methods 25, 249-271.

Wehner D T, Hämäläinen M S, Mody M, and Ahlfors S P, 2008. Head movements of children in MEG: Quantification, effects on source estimation, and compensation. NeuroImage 40, 541-550.

Williamson S J, Pelizzone M, Okada Y, Kaufman L, Crum D B, and Marsden J R, 1985. Five channel SQUID installation for unshielded neuromagnetic measurements.

In: Weinberg H, Stroink G, and Katila T, editors, Biomagnetism: Applications & Theory, pages 46-51. Pergamon, New York.

Williamson S J, Wang J Z, and Ilmoniemi R J, 1989. Method for locating sources of human alpha activity. In: Williamson S J, Hoke M, Stroink G, and Kotani M, editors, Advances in Biomagnetism, pages 257-260, New York. Plenum.

Zimmerman J E, Thiene P, and Harding J T, 1970. Design and operation of stable rf-biased superconducting point-contact quantum devices, and a note on the properties of perfectly clean metal contacts. J Appl Phys 41, 1572-1580.